Friedrich-Schiller University Jena

Faculty of biology and pharmacy
Department of pharmaceutical technology

Diploma thesis

Characterization of non-viral vectors for gene transfer:

Evaluation of size investigations through dynamic light scattering (DLS) to characterize various plasmid/non-viral vector associations

Submitted by: Katharina Leucht
Matriculation number: 64292

Structure

Preface

The experimental part preceding the present work was carried out in the laboratory of galenic pharmacy of the University of Paris-Sud in Châtenay-Malabry. Due to the cooperation of Prof. Alfred Fahr of the Friedrich-Schiller University in Jena and Prof. Elias Fattal of the university Paris-Sud, I was allowed to perform my experiments in the research group of Prof. Elias Fattal. Thank you for having offered me such a great opportunity.

Additional collaboration with Prof. Yves Fromes made it possible to carry out several preparation and examination processes at the institute of myology of the hospital Pitié-Salpêtrière in Paris.

I would especially like to thank Caroline Roques. The present diploma thesis is associated to her dissertation. She strongly supported my work, fairly commented it and was always willing to constructively discuss the topic.

Further thanks go to the whole work groups of Prof. Elias Fattal and Prof. Yves Fromes as well as to all the helping hands of both of these working sites.

Further thanks go to my family and Martin Weber.

Gera, august 2007 Katharina Leucht

Abbreviations

2-HP-β-CD	2-Hydroxypropyl-β-cyclodextrin
bPEI	Branched polyethyleneimine
CD	Cyclodextrin
CMC	Critical micellar concentration
cryo-TEM	Cryo-transmission electron microscopy
DC-cholesterol	3b-[N-(N',N'-dimethyl-aminoethane)-carbamoyl]cholesterol
DDAB	Dimethyldioctadecyl-ammonium bromide
DLS	Dynamic light scattering
DM-β-CD	Dimethyl-β-cyclodextrin
DNA	Deoxyribonucleic acid
DOPE	Dioleoylphosphatidylethanolamine
DOTAP	N[1-(2,3-Dioleoyloxy)propyl]-N,N,N-trimethylammonium-methyl-sulfate
DOTMA	N-[1-(2,3-Dioleyloxy)propyl]-N,N,N-trimethyl-ammonium chloride
EO	Ethylene oxide
EPO	Erythropoietin
HDL	High density lipoprotein
hG-CSF	Human granulocyte-colony stimulating factor
LDV	Laser Doppler Velocimetry
lPEI	Linear polyethyleneimine
pCMVβGal	Plasmid coding for the bacterial β-galactosidase driven by the human cytomegalovirus promoter
PCS	Photon correlation spectroscopy
PEI	Polyethyleneimine
PEO	Polyethylene oxide
PO	Propylene oxide
PPO	Polypropylene oxide
rM-β-CD	Randomly methylated-β-cyclodextrin
SDS	Sodium dodecyl sulfate
SEC	Size exclusion chromatography
SPE-β-CD	Sulphobutylether-β-cyclodextrin
TAE	Tris-Acetate-EDTA

TEM	Transmission electron microscopy
TM-β-CD	Trimethyl-β-cyclodextrin
U_E	Electrophoretic mobility

Abstract

Within this work, from a large amount of non-viral vectors available for gene transfer, some representative ones were chosen to be associated to the widely used reporter gene pCMVβGal. Polycationic bPEI, single positively charged poloxamine 304 and the non-ionic poloxamer PE6400 were applied as polymeric DNA carrier systems. Further non-polymeric formulations contained non-charged cholesterol or monocationic DC-cholesterol, both solubilized by randomly methylated β-cyclodextrins (rM-β-CD). As dispersants, water, NaCl 0.45% and Tyrode's solution were used. Size investigations of the resulting structures were performed through dynamic light scattering (DLS) to evaluate the utilizability of the technique in such concerns.

It appears that the interaction behavior strongly depends on the physicochemical properties of the applied vector: for bPEI and poloxamine 304, both exhibiting strong electrostatic interactions with DNA, the method accurately describes the samples in various media and concentrations. The interaction potential between the plasmid and its complexation partner is clearly evidenced from the size distribution profiles that are different for DNA alone, the vector alone and the associates of both components. The hydrodynamic diameters of the PE6400, cholesterol or DC-cholesterol containing formulations strongly resemble the ones obtained for DNA alone. Since an overlay between the peaks of pCMVβGal and the vector may exist, the application of DLS as sole technique cannot clearly affirm the existence of interactions for theses dynamic structures.

To round off the investigations, morphological cryo-TEM analysis and ζ-potential measurements were performed in addition.

CHAPTER I – THEORETICAL CONSIDERATIONS

1 Introduction

So far a number of inheritable or acquired human pathologies such as genetic diseases, carcinomas and several infections are hardly treatable by conventional medicine. For those, the up-to-date therapeutic concept of gene therapy is expected to be a promising approach. Currently, the lack of efficient and non-toxic gene delivery systems constitutes a major hurdle to the successful application of that method. Hence, many efforts to improve the characteristics of the vectors were attempted and further examinations still continue on a grand scale.

After administration, plasmid DNA (pDNA) has to overcome several barriers before reaching the nucleus of cells, where it finally needs to be expressed [1]. Since DNA is considered to be a large, fragile molecule, therapeutic genes must be protected from extra- and intracellular degradation by nucleases. Due to their size, their negative charge and the resulting hydrophilicity, plasmids further require to be formulated to facilitate their intracellular entry. Besides efforts to administer naked DNA through direct injection, particle bombardment [2, 3] or electroporation [4, 5], numerous gene delivery systems were introduced and evaluated. All those need a significant and reproducible characterization and their quality must be guaranteed by appropriate methods.

For some representative examples of the variety of vectors we investigated the size distribution profiles through dynamic light scattering (DLS; also called photon correlation spectroscopy, PCS). The technique was chosen, since it constitutes a fast and simple method to measure the vector/DNA associations' hydrodynamic diameters. We evaluated the utility the method for different gene delivery systems and examined its advantages and limits depending on the physicochemical properties of the formulations. To give a broad overview, we applied polymeric and non-polymeric systems. The polymers included a polycation, a single positively charged molecule and a non-charged compound, whereas the non-polymeric formulations contained non-charged cholesterol or a single positively charged cholesterol derivative that were solubilized by randomly methylated β-cyclodextrins (rM-β-CD). These vectors were associated to a widely used reporter gene, pCMVβGal, and characterized in different dispersants. Furthermore, we looked at other suitable techniques like zeta (ζ) potential measurement and cryo-transmission electron microscopy (cryo-TEM), providing additional information to complete our investigations.

2 Gene transfer

A lot of approaches concerning the development of gene delivery vectors have been assessed. Those systems can be mainly divided into viral and non-viral vectors.

2.1 Viral vectors

DNA as well as RNA viruses own special molecular mechanisms to transfer their genomes into the nucleus of the infected cells. Thus, they provide an opportunity to transport genetic material within an organism *in vivo* or cell cultures *in vitro*. Retro-, adeno-, adeno-associated and herpes simplex viruses are commonly used examples. Due to their relatively high efficiency for both, DNA delivery and expression [6], they were widely investigated. Viral systems are still involved in many clinical trials, principally concerning cancer therapy [7, 8]. However, the DNA carrying capacity of viral vectors is restricted. Most of the systems cannot transport more than 10kb of exogenous DNA whilst the size needed to deliver complete loci can comprise over 100kb [9]. Recently, viruses that offer a larger gene carrying capacity have been introduced [9, 10], but further limitations including toxicity, potential immunogenicity, high costs and difficulties in production and packaging led to an increasing interest in non-viral vectors in basic and clinical research [6].

2.2 Non-viral vectors

Non-viral vectors can be classified into two main groups: lipids and polymers. Most of the synthetic gene delivery agents currently under development are positively charged to permit interactions with the phosphate backbone of DNA molecules which is deprotonated at physiological pH. Such non-viral systems offer a large diversity. Further variety exists due to the large number of available compositions and to the different methods of preparation. Moreover, synthetic vectors display no size limitation for the transgene and show relatively low immunogenicity. Toxicity depends on the used system as well as on its formulation.
However, until now no system was introduced that approximately reaches viral vector's efficiency. Therefore, current investigations are focused on the improvement of existing formulations and the development of new approaches.

2.2.1 Polymeric carrier systems

Polymer-based vectors principally offer high diversity. From a great number of polymers that are available, we examined the following ones as models for gene delivery reagents of different charges: as a strongly positive charged molecule, branched polyethyleneimine was considered. Poloxamine 304, a so called Tetronic® macromolecule, was investigated since it displays one protonated amino group at a physiological pH and finally, poloxamer PE6400, a Pluronic® block copolymer that owns a non-ionic, amphiphilic structure, was examined as a non-charged compound.

2.2.1.1 Polyethyleneimine (PEI)

In gene delivery, polyethyleneimine (PEI) is mainly applied in two forms: as a branched (bPEI) and as a linear (lPEI) one. Depending on the linkage between the monomers, different structures occur. The branched isomer is synthesized by polymerisation of aziridine molecules, the linear one by cationic ring opening polymerisation of non- or 2-substituted 2-oxazolines and subsequent hydrolysis of the corresponding N-substituted polymer [11, 12]. For several tissues, bPEI as well as lPEI have demonstrated some efficiency *in vitro* as well as *in vivo* [13]. bPEI has been the first cationic polymer reported as a vector for gene therapy. Since it has been extensively characterized in literature and as it is still used as a reference in many studies, we chose the compound as a model for highly positive charged systems. For its structure see figure 2.1.

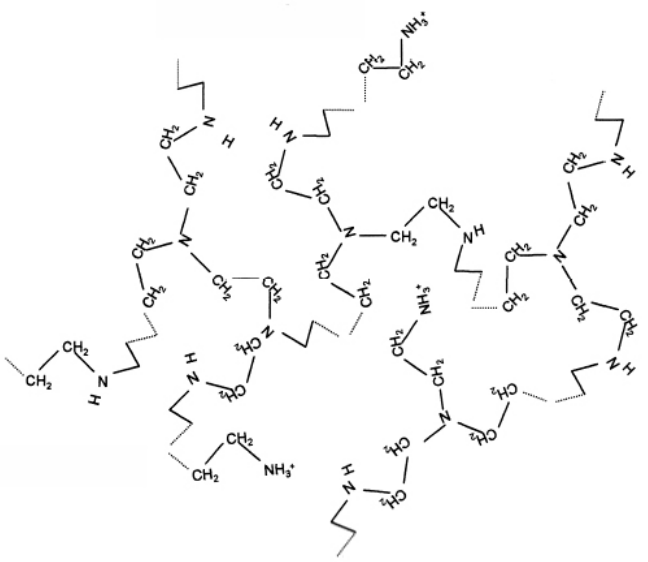

Figure 2.1: Chemical structure of branched PEI (adapted from *Godbey et al.* [11]).

The high density of positive charges leads to PEI's capacity to spontaneously complex DNA. Polyelectrolyte complexes, formed mainly through electrostatic interactions between polycations and DNA, are called polyplexes. Their transfection efficiency depends on material properties as the molecular weight [14] and on complex characteristics such as the ratio between positive and negative charges (N/P ratio), DNA concentration and the method of preparation [15]. All those factors affect the particle size as well as the ζ-potential, which themselves are influencing transfection efficiency [16].

Only cationic amino nitrogen will be involved in the electrostatic interactions between PEI and the negatively charged phosphate residues of the DNA backbone. The N/P ratio describes the ratio of PEI nitrogen atoms to DNA phosphates and hence indicates the amount of polymer used to form the complexes [16]. *Boussif et al.* found the N/P ratio of 9 to be most promising, since they obtained best transfection efficiency under such conditions [15]. As it was demonstrated, about every 6th nitrogen atom of bPEI is protonated under physiological conditions. A ratio of 9 would indicate a mean cationic charge excess of about 1.5, whilst such low charge densities have been shown as favorable for *in vivo* considerations [15, 17]. Since those first experiments, several ratios have been tested and classically, in the literature, an N/P ratio between 6 and 10 is used.

PEI/DNA polyplexes enter cells via endocytosis [18]. PEI contains primary, secondary and tertiary nitrogen atoms, whereof each can be potentially protonated. This leads to a high buffering capacity in the endosomal environment over a wide range of pH [15]. Thereby, osmotic swelling of the vesicles is caused, which finally leads to their rupture and to the polyplexes' release into the cytoplasm. This mechanism avoids the fusion of endosomes with lysosomes and hence protects DNA from being exposed to lysosomal DNase degradation [16]. The described mechanism of endosomolysis is well known as 'proton sponge' hypothesis [19].

When first reported as gene delivery vectors, PEI/DNA complexes were examined to display low *in vitro* toxicity. Whilst an N/P ratio of 9 was determined as favorable concerning transfection efficiency, only very positively charged complexes (N/P > 90) showed cytotoxic properties [15]. Nevertheless, permeabilizing effects of PEI on Gram negative bacterial outer membranes [20] and restricted cell function and viability [12] were described later. Recently, *Boeckle et al.* showed that unbound PEI contributes to cellular and systemic toxicity [21]. They used size exclusion chromatography (SEC) to purify PEI from the uncomplexed compound which led to decreased toxic effects *in vivo* and *in vitro*. In contrast, they

demonstrated free PEI to influence the vector's transfection efficiency positively, since it was increased when such non-complexed molecules were present.
Gharwan et al. investigated bPEI for intrauterine gene delivery into livers of fetal mice in the last trimester of pregnancy [22]. For bPEI/DNA complexes at an N/P ratio of 6, only 24% of the fetuses survived the treatment. However, it must be kept in mind that delivery into fetuses always causes additional problems and that it is even more delicate than any other way of administration. After having injected polyplexes at a N/P ratio of 10 into the pericardial sac of wild type Syrian hamster, 5 of 6 animals died within one hour [23]. These findings indicate that *in vivo* PEI cannot be regarded as a little-toxic non-viral vector.

As low cationic charge density should be favorable for *in vivo* experiments, monocationic and non cationic polymers were investigated and evaluated as gene delivery systems. Thus poloxamines and poloxamers, two families of amphiphilic surfactants used in several biomedical research fields [24], have been considered for gene therapy.

2.2.1.2 Poloxamines

Also named as N,N,N',N'-tetra[(oxyethylene)-(oxypropylene)]diaminoethylenes, ethylene diamine alkoxylates or Tetronics® [25], poloxamines comprise a group of amphiphilic tetrafunctional AB block copolymers. Their chemical structure shows a central ethylene diamine, whereof each nitrogen atom is connected to two blocks consisting of polymerized ethylene oxide (EO) and propylene oxide (PO), respectively. Polyethylene oxide (PEO, the A-block) appears as particularly hydrophilic, whereas polypropylene oxide (PPO, the B-block) forms the more hydrophobic part of the molecule. Their general structure is described on figure 2.2.

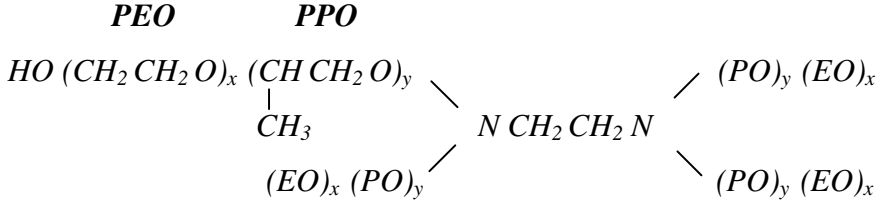

Figure 2.2: General molecular structure of poloxamines (adapted from *Moghimi and Hunter* [24]).

Even though such compounds are usually considered as non-ionic surfactants, at physiological pH one of the nitrogen atoms is protonated, generating a mono cationic charge [25]. Several poloxamines that vary in both the PPO and PEO chain's length are available, leading to different molecular weights of the polymers. They range from 1,650 to 30,000Da which results in diverse surfactant consistencies such as viscous and oily or solid and amorphous characteristics [25].

As amphiphilic copolymers, poloxamines spontaneously aggregate in aqueous solutions after having exceeded the critical micellar concentration (CMC). Nanosized colloids are formed, which feature a hydrophobic core surrounded by a hydrophilic shell [26] and can therefore be used as carriers for poorly water soluble or amphiphilic drugs. For poloxamine T701 [25] and T904 [27], micellization is facilitated after deprotonation of the central diamine group. In this case coulombic repulsion forces among the positively charged molecular centers are strongly decreased and thus, they cannot hinder aggregation. However, an increase of the pH-value is not the only possibility to promote micellization. Further opportunities to minimize the hydrophilic properties of the copolymers and thereby to increase aggregation tendency are a rise of temperature and an augmentation of ionic strength. Added ions shield electrostatic repulsion and cause a small salting-out effect which diminishes poly(ethylene oxide) block's hydrophilicity and promotes hydrogen bonding interactions [27].

Besides the described range of application, poloxamines were recently investigated as potential gene delivery systems. At physiological pH, the single positive charge of poloxamines allows interactions with polyanionic DNA molecules [28, 29]. Complexation happens due to electrostatic forces, whereas hydrogen bonding and hydrophobic interactions are involved as well. Poloxamines may be directly associated to DNA or after adsorption onto nanoparticles through its hydrophobic PPO segments [30, 31].

When using a Tetronic® compound of relatively low molecular weight (poloxamine 304) to directly complex DNA, the formation of negatively charged DNA/poloxamine 304 nanospheres takes place. *In vivo* comparison to the transfection efficiency of naked plasmids demonstrated luciferase expression to increase by 17 or 30-fold when 5 or 10% (w/v) of poloxamine 304 is present in the formulations [29].

Within our work, such direct association of vector and DNA was of interest. Thus, we concentrated on formulations as used by *Pitard et al.* and focused on Tetronic® 304 which was examined by them as the best DNA complexing agent [29].

2.2.1.3 Poloxamers

Poloxamers or Pluronics® represent a group of non-ionic block copolymers that have already been utilized as excipients in formulations as gels, w/o and o/w emulsions, nanoparticles coated by the polymers or solid blends [32]. Furthermore, they have been evaluated and successfully used in gene therapy [28, 33, 34].

Like poloxamines, poloxamers are composed of relatively hydrophobic PPO and hydrophilic PEO, but arranged in a linear way. The resulting basic A - B - A structure is displayed on figure 2.3.

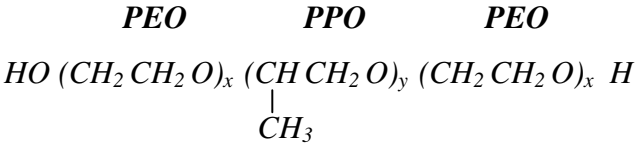

Figure 2.3: General molecular structure of poloxamers (adapted from *Kabanov et al.* [35]).

The number of the blocks' EO and PO units is alterable, leading to variations in the properties of the compound. The synthesis of the polymers can be performed by sequential addition of PO and EO monomers in the presence of sodium or potassium hydroxides as an alkaline catalyzer [32].

Pluronics® exhibit similar aggregation properties as Tetronics® and are able to form polymeric micelles with a core-shell architecture as well. In the same manner, the hydrophobic PPO core is separated from the aqueous solution surrounding the system by its hydrophilic PEO chains that compose the micelle's outer layer. The described structure offers carrying capacities for several therapeutic or diagnosis reagents and thus, increased solubility, improved pharmacokinetic behavior or augmented stability of the incorporated compounds can be reached. Such micellization occurs at polymer concentrations above the CMC. Depending on the PPO and PEO chain's lengths, spherical, rod-like or lamellar structures will be observed. As for Tetronic® copolymers, temperature and ionic strength of the surrounding medium are important factors influencing the structure of the micelles [32].

Poloxamers and DNA are hold together by relatively weak forces such as hydrogen bonding, since the copolymer does not display any charges to permit complex formation due to electrostatic interactions. Examined by *Lemieux et al.,* the non-ionic carrier SP1017, a mixture of the two amphiphilic Pluronic® block copolymers L61 and F127, was shown to increase the

expression of luciferase and β-galactosidase plasmid DNA after intramuscular injection by about 10-fold when compared to naked DNA [28]. Since acute intravenous toxicity occurred to rats at about 5000-fold higher doses [36] than found to be optimal in the reported intramuscular experiments [28], SP1917 formulations were considered as relatively safe. The low amount of DNA, needed to achieve a significant increase in gene expression, is a further advantage, as it will lead to a low extent of unwanted immune response.

Later, Pluronic® PE6400, another block copolymer of the poloxamer family, was reported to be efficient as an *in vivo* promoter of gene delivery to skeletal and cardiac muscles [33]. The level of plasmid expression was comparable to the one reached via electrotransfer, a method that had already been applied successfully to muscles before [4]. In comparison to the results obtained with naked DNA, luciferase activity was increased by 20 to 30-fold after having injected formulations containing 0.05 to 0.5% (w/v) of PE6400 [33]. Further experiments describe the inducible production of erythropoietin (EPO), a glycoprotein hormone, by using intramuscular injection of PE6400/DNA formulations [34]. The hematocrit increased up to 75% and when compared to control mice, the EPO expression rate was 10-fold higher. The augmented number of red blood cells lasted up to 4 months.

As it seems to be an auspicious gene delivery vector, we chose PE6400 as a model of non-ionic polymer for our investigations.

2.2.2 Lipid carrier systems

Lipid-based gene delivery vectors are colloids as liposomes and lipid emulsions [37, 38].

Felgner et al. were the first to use a synthetic, cationic lipid, N-[1-(2,3-dioleyloxy)propyl]-N,N,N-trimethyl-ammonium chloride (DOTMA), to carry genes into cells through liposomal delivery [39]. Since then, different research groups tested a great amount of lipids and further efforts for grading up transfection efficiency were made. Although liposomes in neutral and anionic forms are considered to be less toxic than their cationic counterparts, attention has been focused on positively charged formulations, due to their higher transfection and gene expression rate. A non-negligible disadvantage concerns the little stability of liposome-DNA complexes since liposomal formulations have been shown to aggregate or flocculate after addition of DNA molecules [40]. Therefore, the higher stability of lipid emulsions is seen to be a beneficial property for their use as non-viral vectors. They are well producible in an industrial scale and appear stable during storage [37].

Both systems displayed interesting results *in vitro*, but liposomes as well as DNA/lipid complexes often exhibit reduced transfection efficiency *in vivo* [41]. Furthermore, several toxic effects have been reported. As an *in vitro* example, lipoplexes containing dimethyldioctadecylammonium-bromide (DDAB), dioleoylphosphatidylethanolamine (DOPE) and the commercial transfection-reagent DOTAP (N[1-(2,3-dioleoyloxy)propyl]-N,N,N-trimethylammonium-methylsulfate) were shown to exhibit cytotoxic features to the human carcinoma cell line CaSki, including cell shrinking, mitosis number reduction and vacuolization of the cytoplasm [42].

2.2.2.1 Cholesterol as helper lipid in gene therapy

When compared to viral vectors, the relatively low transfection rate of liposomal systems remains problematic. Adding cholesterol, a micelle forming helper lipid [43], to the formulations, is one approach to ameliorate their efficiency. *Köster et al.* found that cholesterol containing DOTAP liposomes display 2.8-fold higher transfection efficiency in the human breast cancer cells line T-47D than their conventional counterparts [44]. According to them, other steroids exhibit similar effects, since they act through intracellular steroid receptors migrating from the cytosol to the nucleus upon activation. Thus, the transfected DNA might be co-transported to the nucleus. Even though cholesterol does not activate such specific intracellular receptors, it shifts the exogenous DNA from the cytosol to the nucleus. It is well known that membrane fluidity is influenced by its cholesterol content which could be seen as one reason for the enhancement of efficiency. Furthermore, cholesterol is commonly added to liposomes since it stabilizes the lipoplexes, protects them from serum influences and, thus, increases their *in vivo* transfection rate [45]. *Liu et al.* reported that cationic, multilamellar vesicles which incorporate cholesterol as neutral helper lipid increase the efficiency of cationic liposome:DNA complexes [46]. Using the luciferase reporter gene, they found a 1.7-fold increased expression rate, whilst it was even augmented by 569-fold when testing human granulocyte-colony stimulating factor (hG-CSF). Thereby, the latter value corresponds to prolonged circulation time of the liposomal system and to augmented uptake and retention in tissues. The level of gene expression in the lung was significantly higher than in the liver, indicating strong tissue dependence.

As cholesterol and its derivatives are hardly soluble in aqueous solution, *Lawrencia et al.* added cyclodextrin (CD) solubilized 3β-[N-(N',N'-dimethyl-aminoethane)-carbamoyl] cholesterol (DC-cholesterol) to their liposomal DOTAP formulations [47]. After the

incorporation of a pCMVβGal reporter gene into the murine urothelial cell line MB49, *in vitro* transfection efficiency increased by 3.8-fold compared to DOTAP alone. Thereby, in the presence of randomly methylated β-CD (rM-β-CD) and cholesterol, the majority of the complexes were detected in the nucleus, but they were also located in the cytoplasm. When DOTAP alone was used, the plasmid was only found in the cytoplasm, indicating the presence of rM-β-CD/cholesterol influence the escape of DNA from endosomes and to facilitate nuclear uptake. *In vivo,* DOTAP itself did not show efficient transfection of bladder epithelia. In contrast, after intravesical introduction of the formulations containing rM-β-CD/cholesterol into mice's bladders, β-galactosidase activity was detectable up to 30 days. Since exposure of cells to rM-β-CD/cholesterol before transfection via DOTAP/DNA systems led to improved efficiency as well, the beneficial effect of the investigated complexes may be primarily due to an increase of membrane fluidity and permeability.

Particularly the last approach seems very interesting and we chose to investigate cholesterol within our work. It had to be solubilized by CDs as described before [44, 47]. We decided to examine the complexes' properties not only in regard to several dispersants, but also to differently charged derivatives of the molecule. Thus, cholesterol was chosen as a non-ionic compound as well as DC-cholesterol which displays a single positive charge and may therefore show enhanced interaction potential with the anionic phosphate backbone of DNA. For their chemical structures see figure 2.4.

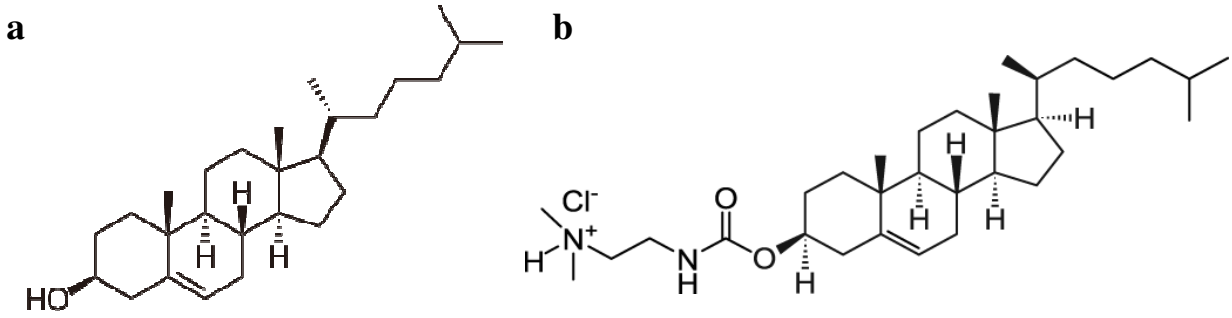

Figure 2.4: Chemical structures of a) cholesterol and b) DC-cholesterol (adapted from Avanti Polar Lipids).

Since CDs constitute an important factor in such investigations, they will be now discussed in detail.

2.2.3 Cyclodextrins

CDs comprise a family of cyclic oligosaccharides, whereof several members are widely-used for pharmaceutical concerns as well as in different sectors like agriculture, food industry and cosmetics [48]. The three natural molecules, α-CD, β-CD and γ-CD, are respectively built up from 6, 7 or 8 D-(+)-glucopyranose subunits. The chemical structure of β-CD is shown in figure 2.5a. Generated by degradation of starch via the enzyme glucosyltransferase, they are linked by α-(1,4)-glycosidic bonds [48] and form conically shaped cylinders (see figure 2.5b). As a consequence of the described conformation, all the primary hydroxyl groups are located at the narrower of the two ring borders, whereas all the secondary ones are placed on the wider side (figure 2.5c) [49]. All these hydrophilic groups are orientated towards the outer surface of the molecule, whilst oxygen atoms, forming hydrogen and glycosidic bonds, point within the cavity. Accordingly, a water compatible exterior and a hydrophobic pore are generated [48, 50]. In figure 2.5d, the approximate dimensions of natural CDs are shown [49].

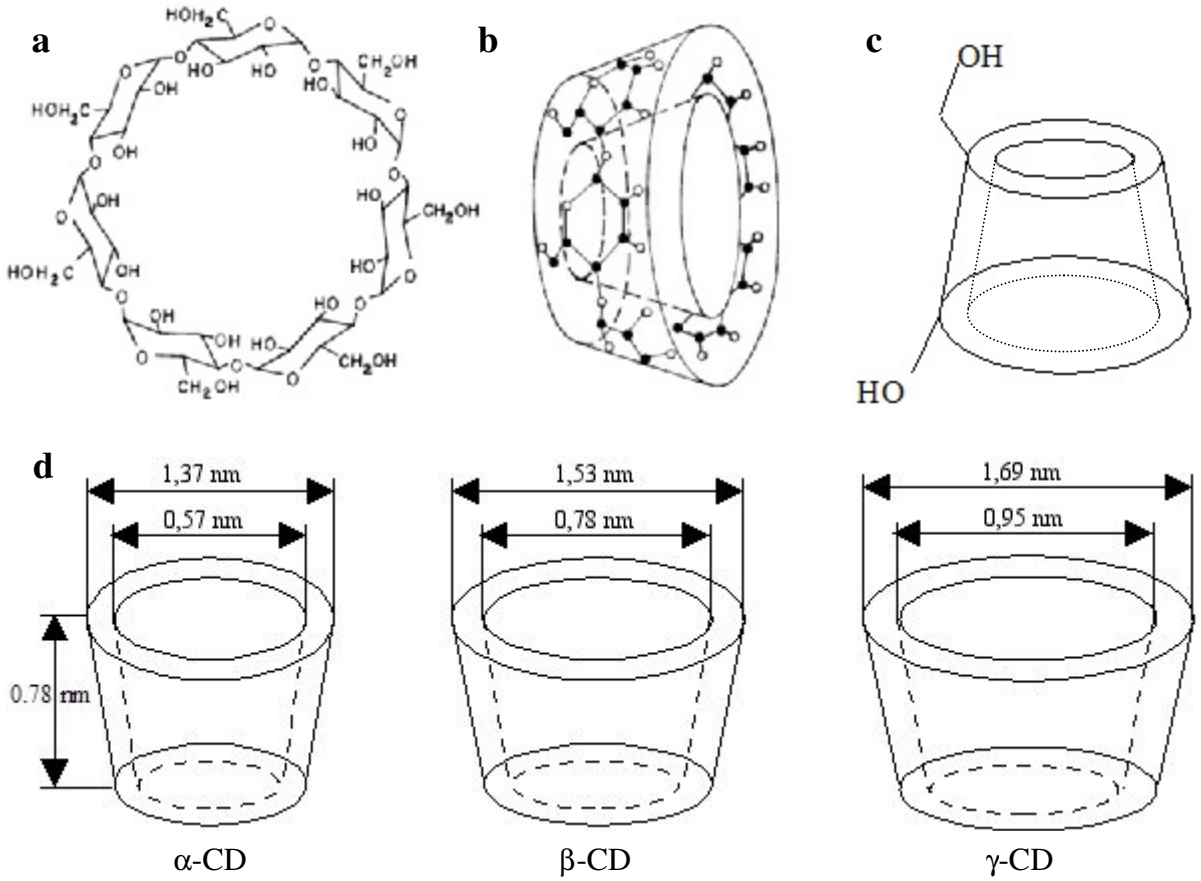

Figure 2.5: Schematic representation of β-CD: a) chemical structure, b) toroidal shape (both adapted from *Challa et al.* [51]) and c) constitution of primary and secondary OH-groups (adapted from *Davis and Brewster* [52]). d) Geometric dimensions of α-, β- and γ-CD (adapted from *Szejtli* [49]).

Due to their unique structure, cyclodextrins are able to form inclusion complexes with various compounds or at least with some of their hydrophobic parts. When dissolved in an aqueous solution, the cavity of CDs is filled with polar water molecules, resulting in an energetically unfavorable state. For this reason, water can be easily substituted by less hydrophilic compounds, so called guest molecules, and without covalent linkages inclusion complexes are formed. Several host-guest ratios, like 1:1, 1:2, 2:1, 2:2, etc., are possible. Association and dissociation of CDs and their guests can be described by the thermodynamic equilibration (1), where G symbolizes the guest molecule and CD·G illustrates the complex.

$$CD + G \rightleftharpoons CD \cdot G \tag{1}$$

For a G:C ratio of 1:1, the complex stability constant K is calculated by equation (2).

$$K_{1:1} = \frac{[CD \cdot G]}{[CD][G]} \tag{2}$$

Low water affinity of several drugs often causes problems in their administration. After having discovered that compounds can be dissolved easier when cyclodextrins are added to the solutions, their disposition to increase the apparent solubility of lipophilic drugs was widely analyzed. The cavity size of α-CD is insufficient for the majority of drugs and γ-CD is expensive. Hence, β-CD was widely used in the earlier stages of pharmaceutical applications, although its water solubility is quite low (18.5 g/l) compared to the α- and the γ-derivates (145 and 232 g/l, respectively) [49, 51]. As a reason, the formation of an intra-molecular hydrogen bond network between the secondary hydroxyl groups is mentioned. Substituting some of these functional elements leads to an increased solubility, which is caused by disruption of the responsible linkages. Such chemically modified CDs are the results of etherification or introduction of other functional elements at the three hydroxyl groups of each glucose subunit. The methylated derivates dimethyl-β-CD (DM-β-CD), trimethyl-β-CD (TM-β-CD) and randomly methylated β-CD (rM-β-CD) as well as 2-hydroxypropylated β-CD (2-HP-β-CD) and sulphobutylether-β-CD (SPE-β-CD) are just some examples for available molecules [48]. Several formulations containing cyclodextrins and utilizing their solubilizing effect are already introduced onto the market. Thereof the following shall be mentioned exemplarily: Nicorette®microtab (Nicotine, sublingual tablet, containing β-CD, [53]), Aerodiol® (17β-Oestradiol, nasal spray, rM-β-CD, [54]) and Voltaren®ophta CD (Diclofenac

sodium, eye drops, 2-HP-γ-CD, [55]). Further examinations also consider their use in peptide, protein and oligonucleotide delivery [51].

To study CD inclusions complexes, the phase solubility method of *Higuchi and Connors* [56] has been widely used. By this approach, the effect of the solubilizer, CD in our case, onto the drug being solubilized, e.g. cholesterol, is examined [51]. Such phase solubility diagrams are obtained as follows: excess amounts of the guest molecule are added to a constant volume of aqueous solutions containing increasing concentrations of CDs. After reaching the equilibrium, the non-solubilized drug molecules are removed and the amount of the dissolved guest molecules is determined.

This phase solubility method allows the description of two types of curves: an A type, denoting the formation of soluble complexes, and a B type for the less soluble ones. Both are divided into several subtypes: the A curves are classified into A_L systems, signalizing linear increase of drug solubility as a function of CD concentration, and further into A_P and A_N subtypes for positively or negatively deviating isotherms. B_S curves indicate limited solubility, whilst complexes showing B_I behavior are insoluble. An illustration is given on figure 2.6.

Due to its low solubility, β-CD often gives B type curves, whereas α- and γ-, as well as chemically modified CDs like rM-β-CD mainly show A type behavior [51]. When following an A_L or A_N comportment, drugs will not precipitate through dilution of the formulations. In contrast, a precipitation of the CD's guest molecule may occur if an A_P correlation between drug solubility and CD concentration exists.

By this method, stoichiometry of guest/CD complexes and the numeric value of their stability constant can be obtained, indicating the technique as very useful in such complexes' characterization.

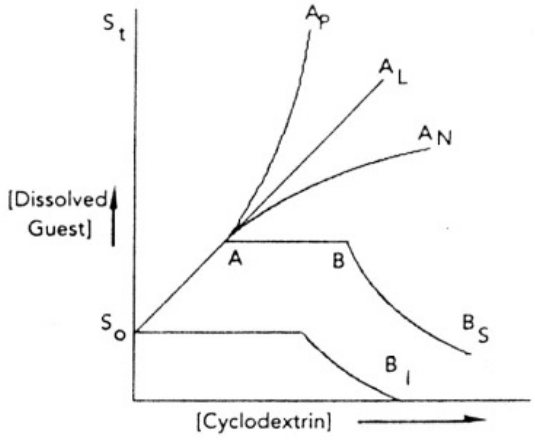

Figure 2.6: Theoretical phase solubility diagram (adapted from *Challa et al.* [51]). S_O symbolizes the intrinsic solubility of the drug studied under the conditions.

CDs as well as their complexes show self-association in solution and form aggregates of two or more CD molecules or complexes, respectively. During the last 15 years, this phenomena has been studied and proved by several methods [57-60], whereas *Coleman et al.* were the first to report the existence of assemblies of natural CDs after DLS investigations [57].

González-Gaitano et al. [58] also used DLS to study the association of CDs themselves, without the presence of guest molecules. According to their investigations, for rM-β-CDs aggregates of 120nm and monomers of 1.7nm were found. Such an assembly takes place very fast. The aggregation tendency of this methylated CD derivative was less obvious than for non-substituted CDs. It was concluded that such an assembly is associated with the presence of free OH groups at the rims of the CD molecules.

Recently, a further study of β-CD's aggregation behavior was published, using cryo-TEM and DLS [59]. As for the DLS examinations, a 3mM (0.34% w/v) sample as well as samples of 9 (1.02% w/v) and 12mM (1.32% w/v) showed a mean hydrodynamic diameter of about 180nm. Several samples accessorily displayed some particles as large as a few micrometers. Cryo-TEM experiments of 3mM solutions pointed out the existence of small globular particles with a mean diameter of about 6nm. These particles can form aggregates, displaying a branched appearance. Furthermore, disc-shaped structures were detected in the formulations, whereof some showed connections to each other via their edges.

Loftsson et al. used the phase solubility method as described above to characterize CDs complexes [60]. They tested several CD derivatives combined with different molecules to be solubilized. Cholesterol showed highest affinity for the most hydrophobic of the investigated CD derivatives such as rM-β-CD. Thereby, such a host-guest combination is of particular interest in our work. The curve for cholesterol associated to rM-β-CD cavities was found to show a positive deviation from linearity and thus, an A_P profile was suggested. These results indicate the formation of higher-order inclusion complexes.

CDs are known to interact with biological membranes and to display the opportunity of modifying their cholesterol content. They are able to remove phospholipids [61] and proteins [62] from cell membranes, but *in vitro* mainly a high affinity for cholesterol was reported [63]. Especially β-CD was mentioned to own relative selectivity for cholesterol, leading to the idea of using these compounds as effective modulators of cholesterol metabolism *in vivo* [63]. By the application of CD formulations, a cholesterol efflux from membranes may occur, rending such biological barriers more permeable. *Kilsdonk et al.* [63] examined 10mM β-CD, 2-OH-β-CD and rM-β-CD, respectively, to induce the release of 50-90% of L-cell cholesterol within 8h of incubation. They stated CDs to be more efficient cholesterol acceptors with high

potential for each investigated cell type than high density lipoprotein (HDL). The theory of cholesterol molecules that desorb from a membrane and diffuse directly into the hydrophobic cavity of CDs without total desorption into the aqueous environment, may serve as an explanation [61]. For incorporation into HDL, complete transfer into the aqueous phase, a diffusion step and final solubilization by the acceptor molecule is necessary.

Since exhibiting cell toxicity due to resulting membrane instability, such decline of membrane's cholesterol content can be seen as a disadvantage. However, in gene therapy it may also constitute a chance to facilitate the entry of DNA into cells. *Christian et al.* described further interesting observations [64]. They used CD/cholesterol complexes to modify cell cholesterol content and reached net depletion as well as net enrichment. For rM-β-CD, the membrane's sterol amount was not modified when solutions of a molar rM-β-CD/cholesterol ratio of 8:1 were applied. When saturated with cholesterol, the CD formulations exhibited cell cholesterol increase, whilst, when containing less cholesterol, a diminution occurred that renders the membranes more permeable.

Polymeric derivates of cyclodextrins are widely used as CD containing formulations for gene transfer. Two main types are applied: polymers prepared with non charged CDs, complexed to an ionic guest molecule acting as a linker between the CD polymer and DNA (see figure 2.7) [65, 66], and polymers based on polyamino derivates of CD, displaying positive charges themselves [67].

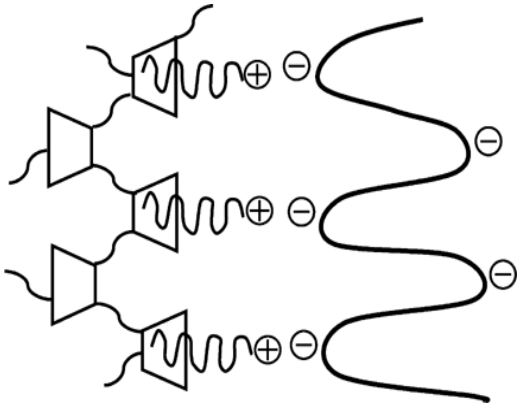

Figure 2.7: Schematic representation of ternary complex formation between poly-βCD, a cationic guest molecule and DNA (adapted from *Galant et al.* [66]).

But also monomeric CDs have already been reported as gene delivery vectors, an approach that will be referred to in our work [47].

For all therapeutic concepts, safety represents a primary concern and toxicological studies are of major interest. Prior examinations demonstrated mainly the parent CDs to be hemolytic [63] and nephrotoxic [62]. As the kidney remains the main elimination organ of CDs from systemic circulation, they are concentrated in the proximal tubule after glomerular filtration. Thereby, the nephrotoxicity corresponds to a series of variations in the vacuolar organelles of the proximal convolute [62]. As variations of CD's hydroxyl substituents may result in increased hydrophilicity and greater solubility, such derivatives exhibit reduced renal toxicity. Concerning methylated CD derivates, *in vitro* toxicity was assessed for several cells types. Administered on a buccal way, rM-β-CD shows increasing toxicity as concentration and time exposure were heightened, but can be considered as relatively safe when used at levels below 5% (w/v) [68]. In an intestinal cell culture model, DM-β-CD exhibited insignificant toxicity for the human colorectal carcinoma cell line Caco-2 [69]. Furthermore, *in vitro* safety of nasal formulations containing CDs as an absorption enhancer could be confirmed [70]. Since *in vitro*, influencing factors such as drainage, dilution and systemic conjunctival absorption are absent, and *in vivo*, administration is generally seen to be more complex, the described indication is not directly assignable to *in vivo* conditions.

3 Characteristics of the applied techniques

3.1 Dynamic light scattering (DLS)

To analyze the size distribution of several nanosized therapeutic systems, DLS measurements may be applied. In liquids, every particle underlies a casual movement into the three directions in space, intensified by effects due to collision with and repulsion by their surrounding molecules. Such behavior is called the Brownian motion. Thereby, small particles move faster than large ones, permitting the calculation of the hydrodynamic diameter of the sphere that diffuses light as fast as the particle being measured. The principle is based upon irradiating the particles by a laser and analyzing the intensity variations of the scattered light. Size and Brownian motion are related by the equation of Stokes-Einstein (3), whereas the hydrodynamic diameter of the particle (d) may be calculated by its inverse proportionality to the coefficient of diffusion (D).

$$D = \frac{k_B T}{3 \pi \eta d} \tag{3}$$

k_B represents the Boltzmann constant ($k_B = 1.38 \cdot 10^{-23}$ J/K), T marks the absolute temperature and η describes the dynamic viscosity. Within the instrument, a digital correlator is included which basically measures the degree of similarity of two signals over a certain time segment and displays a correlation function. From these measurements, the apparatus calculates the diffusion coefficient of the particles in the sample. Hence, their hydrodynamic diameter may be derived [71, 72]. A scheme of the measurement principle is given on figure 3.1.

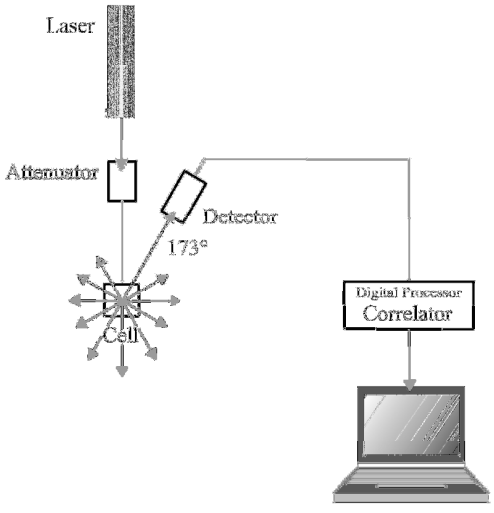

Figure 3.1: Scheme of the DLS measurement principle (adapted from Malvern, Zetasizer nano users manual).

The Z-average size (also called as the cumulants mean) is the most stable parameter produced by the DLS technique. It is only usable and comparable to other techniques if the sample is monomodal (displaying only one peak), spherical, and monodisperse. The cumulant analysis gives access to a mean size value and a width parameter (polydispersity index, PDI). The Z-average size is likely to be interpreted incorrectly if the distribution is broad and the system displays high polydispersity. For low polydispersity (< 0.1) the cumulant analysis will give a good description, well comparable to other techniques. The results may still be used for comparative purposes when the PDI is increased up to 0.5. At values above 0.5 it is not advisable to rely on the Z-average size.

3.2 Zeta potential (ζ-potential)

The ζ-potential offers a method to describe the apparent net charge of a particle, caused by ionization of the molecules' surface groups. Direct measurement of the Nernst potential, corresponding to the surface charges, is not possible. When introducing a particle in aqueous solution, counter ions will bind to the particle's surface to compensate the potential difference. Thus, a fix electrical double layer (Stern layer) surrounds such particles. Within the outer layer the ions are more diffuse. At a certain distance from the surface a boundary is reached. Within, the ions move with the particle being in motion and beyond, they do not travel with it. The potential existing at this boundary is known as ζ-potential. For a scheme see figure 3.2.

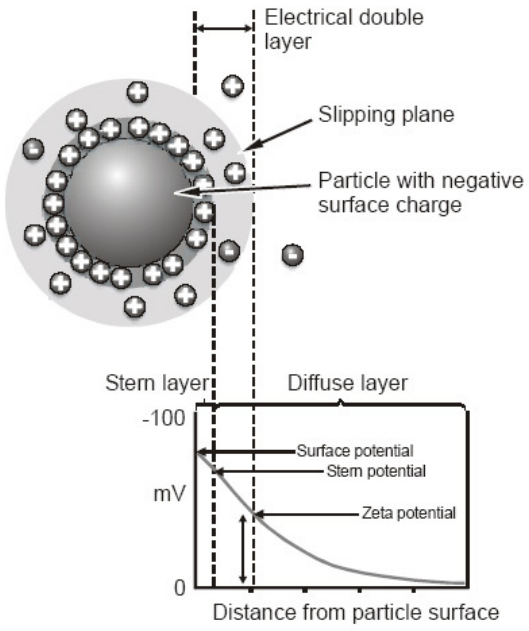

Figure 3.2: Schematic representation of the ζ-potential (adapted from Malvern, Zetasizer nano users manual).

The extent of this potential may serve as an indicator of the stability of a colloidal system, since, when all particles own high positive or negative charges, they exert repulsive forces on each other and are therefore hindered to flocculate or even aggregate. -30mV or +30mV, respectively, are generally seen as borderlines between stable and unstable states.

To measure the ζ-potential, an electric field needs to be applied to the formulations. The particles will be attracted by the electrode of opposite charge, whereas they are kept back by forces due to the surrounding medium's viscosity. When these two processes are equilibrated, the particles move at constant speed (velocity) expressed as electrophoretic mobility (U_E). When applying the Henry equation (4), the ζ-potential can be calculated as follows:

$$U_E = \frac{2\varepsilon\zeta \; f(ka)}{3\eta} \tag{4}$$

Thereby, ε describes the dielectric constant of the sample, ζ marks the ζ-potential, *f* (ka) constitutes the Henry equation and η symbolizes the dynamic viscosity. Since the ζ-potential is commonly obtained from aqueous solutions at moderate ion concentrations, *f* (ka) is indicated as the Smoluchowski approximation and therefore has a value of 1.5 [73, 74].

In our laboratory the Zetasizer Nano ZS (Malvern, Worcestershire, England) is used to perform such measurements. The instrument applies Laser Doppler Velocimetry (LDV) to measure U_E. The incident laser beam gets scattered by the particles dispersed in the liquid. Detected in a 17° angle, the scattered light is related to a reference beam and a fluctuating signal is generated. Its frequency is proportional to the particles' speed and thus, it is characteristic for U_E and the ζ-potential. A scheme of the measurement principle is given on figure 3.3.

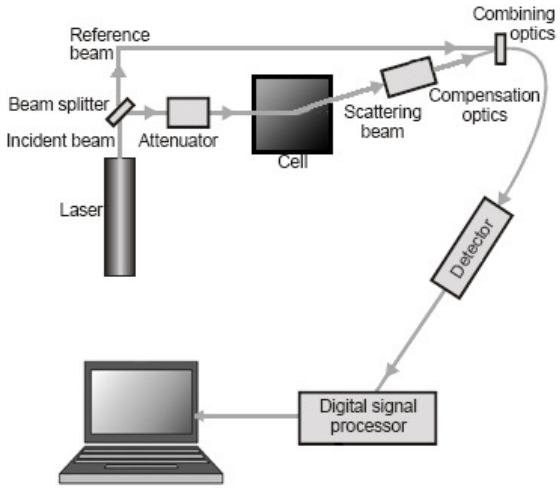

Figure 3.3: Scheme of the ζ-potential measurement principle (from Malvern, Zetasizer nano users manual).

3.3 Transmission electron microscopy (TEM)

Transmission electron microscopy (TEM) offers the possibility to detect surfaces of samples containing structures down to less than one nm in size. A cathode emits electrons that generate a high voltage beam. Since attracted by the anode, the electrons are accelerated in an electric field. Due to the very small wave length of such fast moving electrons, the resolution of electron microscopes is much higher than when using a light optical microscope. The resolution of the latter one is restricted by the shortest wave length of visible light. When applying the transmission mode, the electrons are detected after having passed through the sample. Therefore these samples need to be prepared as a very thin, electron semitransparent film. After magnification of the micrographs, the sample can be analyzed [75].

As dynamic and delicate structures do not support the drying or the staining and fixation steps that are necessary to prepare samples for conventional TEM, cryo-TEM may be used to analyze such formulations.

CHAPTER II – EXPERIMENTAL SECTION

4 Materials and methods

4.1 Materials

Branched PEI (average MW: 25kDa), cholesterol and Tyrode's salt were purchased from Sigma-Aldrich (Lyon, France). The composition of Tyrode's solution is indicated in table 4.1. Sodium chloride solution for infusions (NaCl 0.9% w/v) was ordered from MacoPharma (Mouvaux, France) and Poloxamine 304 (Tetronic® 304) as well as poloxamer (Pluronic® PE6400) block copolymers were provided by BASF (Levallois, France). Randomly methylated β-cyclodextrin (Cavasol® W7 M) was obtained from Wacker Chemie (Burghausen, Germany), DC-cholesterol from Avanti polar lipids (Alabaster, USA) and chloroform from Carlo Erba Reagents (Val de Reuil, France). Water was purified using a Synergy system from Millipore (Molsheim, France).

Table 4.1: Composition of Tyrode's solution (1X).

Salt	Concentration [g/l]
CaCl (anhydrous)	0.2
$MgCl_2$ (anhydrous)	0.1
KCl	0.2
NaCl	8.0
NaH_2PO_4 (anhydrous)	0.05
D-glucose	1.0
$NaHCO_3$	1.0

4.2 Preparation and purification of pCMVβGal

A 7.2kb reporter gene coding for bacterial β-galactosidase (pCMVβGal, Clontech, Saint Quentin Yvelines, France) was used as plasmidic reporter system (figure 4.1). It was introduced in JM109 *E. coli* via thermic shock treatment and amplified by that strain. Purification was performed with the plasmid purification kit NucleoBond® PC EF 10000 as

described by the manufacturer (Macherey-Nagel, Düren, Germany). The system employs an alkaline/sodium dodecyl sulfate (SDS) lysis buffer to prepare the bacterial cell pellet. Via this treatment, chromosomal and plasmid DNA are denatured. By addition of potassium acetate buffer, the lysate becomes neutral and chromosomal DNA as well as other cellular compounds precipitate. Plasmid DNA remains in solution. Purification was carried out by using a NucleoBond® column AX 10000. The column displays a silica-based anion-exchange resin that permits the negatively charged DNA phosphate backbone to bind specifically. Finally, the plasmid is eluted by washing the column with an appropriate buffer. Afterwards, plasmid DNA was precipitated by isopropanol, washed with ethanol and resuspended in water. The final DNA concentration was determined by UV spectrophotometry (NanoDrop® ND-1000 spectrophotometer) and its purity was checked through calculation of the DNA/protein and DNA/benzenes absorption ratios at the wave length of their maximum absorption (λ_{max} (DNA) = 260nm, λ_{max} (protein) = 280nm, λ_{max} (benzenes) = 230nm). Each of three independent samples was measured three times. Furthermore, after digestion of the plasmid with 2 restriction enzymes, a gel electrophoresis was performed at 80mV. The gel was prepared in TAE buffer with 1% (w/v) of agarose (Eurogentech, Seraing, Belgium). EcoR1 (Invitrogen Life Technologies, Cergy Pontoise, France) was used to linearize the plasmid, and Not1 (New England Biolabs, Ipswich, USA) separated its insert from the backbone. As a marker, SmartLadder was applied (Eurogentec, Seraing, Belgium).

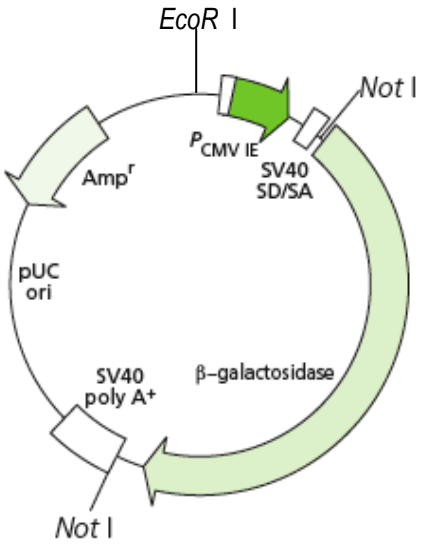

Figure 4.1: Restriction map of pCMVβGal (adapted from Clontech, product information).

4.3 Preparation of the formulations

Unless otherwise noted all experiments were performed at a DNA concentration of 0.13µg/µl.

4.3.1 bPEI / DNA

bPEI complexes were prepared at a final N/P ratio of 10. A bPEI stock solution of 60mg/ml was prepared in DNase and RNase free water. HCl was added until a pH value of 6.9 was reached. Before storage at -20°C, the solution was filtered through a 0.22µm PVDF membrane filter. Since 1µg of DNA contains 3nmoles of anionic phosphate, the volume needed to form the complexes was calculated as follows (equation 5).

$$\mu l \text{ of } b\text{PEI stock solution to be used } = \frac{(\mu g \text{ of DNA} \cdot 3) \cdot N/P \text{ ratio}}{mM \text{ of } b\text{PEI}} \qquad (5)$$

The bPEI molar concentration is expressed as concentration of monomer nitrogen residues. To form the complexes, a suitably diluted solution of bPEI was prepared in water and mixed equivolumetrically with 0.26µg/µl of the plasmids in water, NaCl 0.9% or Tyrode 2X. The samples were mixed by pipetting and by vortexing gently. Before being used, they were allowed to equilibrate at room temperature for at least 30 minutes.

4.3.2 Poloxamine 304 / DNA

Formulations containing poloxamine 304 all displayed a final concentration of 5% (w/v). As previously described by *Pitard et al.* [29], a 20% (w/v) stock solution of the block polymer was prepared in water and stored at 4°C. Before use, this solution was diluted with water to 10% (w/v). Plasmid DNA was suitably diluted in purified water, 0.9% (w/v) NaCl or Tyrode 2X. Afterwards, equal volumes of the DNA and Poloxamine 304 solutions were carefully mixed by pipetting and vortexed gently. Prior to their use, the complexes were given at least 30 minutes of equilibration time at room temperature.

4.3.3 PE6400 / DNA

A stock solution of PE6400 at 2% (w/v) was prepared in water and kept at 4°C until used. The final concentration in the samples was set to 0.05% (w/v). Thus, the stock solution needed to be diluted by water to 0.1% before being equivolumetrically mixed with the DNA solution. The plasmid was prepared in ultra pure water, 0.9% (w/v) NaCl or 2X Tyrode's solution. To

homogenize the samples, they were gently mixed during their preparation by pipetting and vortexed afterwards at relatively low speed. Before performing the measurements, the samples were allowed to equilibrate at room temperature for at least 30 minutes.

4.3.4 rM-β-CD/DNA, rM-β-CD/cholesterol/DNA and rM-β-CD/DC-cholesterol/DNA

If not otherwise stated, the samples contain 0.5% (w/v) of rM-β-CD and the lipid containing systems display a molar ratio of rM-β-CD/cholesterol or rM-β-CD/DC-cholesterol of 15:1.

For rM-β-CD/DNA associations, equal volumes of an appropriately diluted solution of rM-β-CD in water, NaCl 0.9% or Tyrode 2X and a plasmid solution of 0.26µg/µl were gently pipeted and vortexed. The samples were investigated after 30min of equilibration.

The cholesterol or DC-cholesterol containing formulations were prepared as follows: the first step consisted in complexation of the lipids with rM-β-CD. We applied two methods, named #1 and #2, respectively. When using #1, calculated amounts of cholesterol or DC-cholesterol were weighed into a volumetric flask. This one was filled till the gage mark with a solution of rM-β-CD at the desired concentration, prepared by simply dissolving solid rM-β-CD in water. The suspensions were allowed to equilibrate at 25°C during 5 days under magnetic stirring. *Christian et al.* suggested a different method (#2) to obtain such complexes [64] which was adapted as follows: a cholesterol or DC-cholesterol stock solution of 10µg/µl was prepared in chloroform. A suitable volume was taken and chloroform was evaporated at 80rpm within 1.5 hours. (rotavapor R-124, Büchi laboratory equipment, Flawil, Switzerland). Thereby a film of the sterols was formed at the walls of the tube. A solution of rM-β-CD was prepared as described for #1. An appropriate volume of rM-β-CD solution was added to the tubes to redissolve the film of cholesterol or DC-cholesterol. The dried cholesterol was brought off the borders by vortexing the solutions during 30s and by 3min of sonication in a bath sonicator. The tubes were stored overnight in an incubation chamber at 37°C under agitation. DNA solutions of 0.26µg/µl were prepared in water or Tyrode 2X and added to equal volumes of rM-β-CD/cholesterol or rM-β-CD/DC-cholesterol. The samples were mixed via gently pipetting and vortexing and, thereafter, they were allowed to equilibrate for at least 30min.

As indicated later, the formulations were filtered through several filter types, centrifuged at different speed, varied in initial or final rM-β-CD concentration or adapted in rM-β-CD/cholesterol or rM-β-CD/DC-cholesterol ratios.

4.4 Dynamic light scattering (DLS)

The distribution of the complexes' hydrodynamic size was obtained by dynamic light scattering measurement. For our investigations, a Zetasizer Nano ZS (Malvern, Worcestershire, England) was used. The emitted laser light features a wave length of 633nm and the scattered information is detected upon a 173° angle via backscatter detection. For each formulation, the results of at least three separately produced samples, whereof each was measured three times at 25°C, were averaged and expressed as mean ± standard deviation. To compare the mean hydrodynamic size values of different formulations, Student's t-test was applied, setting the level of significance to $p < 0.05$.

For rM-β-CD/DC-cholesterol/DNA associations, stability of the size profile curves obtained from the formulations was further investigated depending on temperature. Therefore, the apparatus was set to perform measurements from 37°C down to 4°C in steps of 3K.

4.5 Zeta potential (ζ-potential)

For our measurements the Zetasizer Nano ZS (Malvern, Worcestershire, England) was used. The apparatus processed the information according to the Smoluchowski approximation. Again, the values were obtained form three samples, all measured three times at 25°C. For each system, the results were averaged and expressed as mean ± standard deviation. Student's t-test was applied to determine, whether two mean values were significantly different from each other or not ($p < 0.05$).

4.6 Cryo-transmission electron microscopy (cryo-TEM)

To obtain a very thin sample film, 5µl of the aqueous solutions are applied to a lacey formvar/carbon copper grid (Ted Pella, USA), that is clamped into a specimen holder. After blotting excess amounts of the formulations, the grid is plunged into liquid ethane, whereas the film vitrifies instantaneously without crystallization. During all the following operations and during the measurement, the specimen has to be kept at liquid nitrogen temperature to avoid thawing. Subsequently, the sample is placed into a cooled transfer unit, inserted into the microscope and examined in transmission mode.

For our investigations we used an EM 912 Omega microscope (Carl Zeiss NTS, Göttingen, Germany), operating at 120kV.

5 Results

5.1 DNA

5.1.1 Verification of the plasmid by gel electrophoresis

After purification of plasmid DNA from *E. coli*, each preparation was submitted to the verification of the plasmid obtained, as well as to the evaluation of its concentration and purity. Verification of the plasmid was performed through gel electrophoresis on intact and enzymatically digested DNA samples. By the help of a molecular weight marker, the quantity of kilo base pairs, building up the investigated plasmid, is assessable. As shown on figure 5.1, intact pCMVβGal (P_{intact}) migrates farther than expected for a 7.2kb plasmid which results from its supercoiled form. As expected, the linearized sample (P_{EcoR1}) has been found between the 6 and 8kb bands of the marker, indicating 7.2kb. As pCMVβGal exhibits two restriction sites for Not1, after digestion of the plasmid by that enzyme (P_{Not1}), two bands corresponding to two DNA fragments were obtained. All those findings confirm the identity of the pCMVβGal reporter gene.

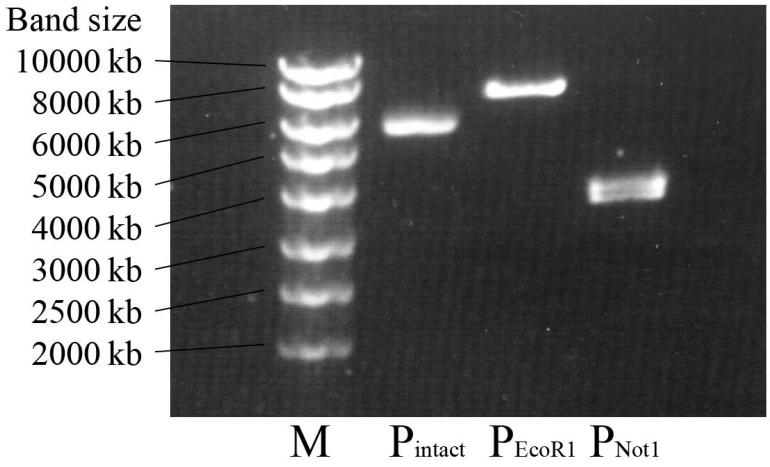

Figure 5.1: Photograph of a 1% agarose gel of pCMVβGal before (P_{intact}) and after digestion by EcoR1 (P_{EcoR1}) and Not1 (P_{Not1}) restriction enzymes to check identity and purity of the plasmid. M = molecular weight marker.

5.1.2 Evaluation of DNA concentration and purity by UV spectrophotometry

After plasmid purification, we reached final DNA concentrations of 4.3 to 7.8µg/µl. Moreover, purity of the samples was confirmed through the absorption ratios of 260nm/280nm and 260nm/230nm. DNA was considered pure when the ratios ranged between 1.8-2.0 and 2.2-2.4, respectively. All our samples correspond to that criterion.

5.1.3 Size of DNA in different dispersants

Prior to the evaluation of the various formulations, naked DNA was investigated through DLS measurements in water, 0.45% (w/v) of NaCl and Tyrode's solution. We worked at a plasmid concentration of 0.13µg/µl. In water and in NaCl 0.45%, laser power was set to 100%, whilst 30 or 100% were applied in Tyrode. In both ion-containing dispersants, the count rate was increased by 3 to 4-fold with reference to water. Moreover, a non-consistent and unstable profile was obtained in water. Several peaks were observed, whose positions displayed great inter- and intraindividual variations. Thus, no mean sizes could be specified. In NaCl 0.45% as well as in Tyrode's solution, more consistent findings displaying two major peaks resulted from the measurements (see figure 5.2). When looking at the size distribution by intensity, the main population showed a mean hydrodynamic diameter of 134nm for both dispersants. Within some measurements, a further peak was detected at about 20nm. Since the PDI decreased from water over NaCl 0.45% to Tyrode, higher homogeneity for DNA in salt containing dispersant was indicated. For the summarized results see table 5.1.

Table 5.1: Results obtained by DLS measurements for naked DNA in different dispersants.

	Dispersant	pH	Peak I [nm]	Peak II [nm]	PDI
DNA	Water	5.8	- *	- *	0.53 ± 0.19
	NaCl 0.45%	6.6	134 ± 13	21.0 ±6.9	0.43 ± 0.04
	Tyrode	8.1	134 ± 6	18.7 ± 2.2	0.35 ± 0.11

* As several unstable peaks were obtained, no mean value may be indicated.

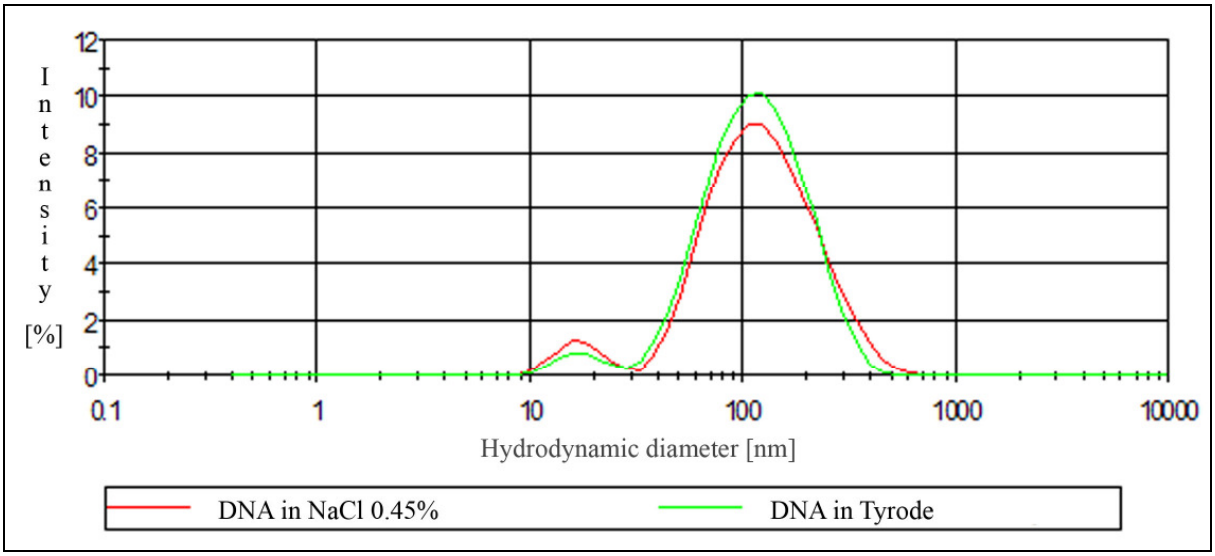

Figure 5.2: Size distribution profile by intensity for DNA at a concentration of 0.13µg/µl in NaCl 0.45% and Tyrode's solution.

5.1.4 ζ-potential of DNA in different dispersants

No significant difference could be observed between the ζ-potential measurements obtained for pDNA in water or in Tyrode's solution (see table 5.2). However, for NaCl 0.45% an even more negative value was obtained. When looking at the phase plot profile, data quality resembled each other for all the three dispersants.

Table 5.2: ζ-potential for naked DNA in different dispersants.

	Dispersant	ζ-potential [mV]
DNA	Water	-25.6 ± 4.2
	NaCl 0.45%	-39.5 ± 2.9
	Tyrode	-27.3 ± 3.8

5.2 bPEI/DNA

5.2.1 Size of bPEI and bPEI/DNA complexes in different dispersants

To serve as a reference, non-complexed bPEI was measured at the same concentration used to form bPEI/DNA complexes at an N/P ratio of 10. For such dilution, laser power was automatically set to maximum transmission. With reference to water, the count rate was increased by 2-fold in Tyrode's solution. After preparation in that dispersant, the main peak of bPEI itself showed a slightly, but non-significantly lower average size when compared to the same peak obtained in water (see table 5.3). Although in water some specimen showed a second population of weaker intensity, the PDI values were found to be similar for both media. All those findings indicate no important size profile changes for bPEI alone depending on the dispersant. Since for water and Tyrode's solution almost the same size intensity profiles were obtained, similar results are expected for NaCl 0.45% and thus, no examinations were carried out for that latter dispersant.

In water, DNA that was complexed by bPEI exists as particles of 86.7 ± 2.6nm in hydrodynamic diameter (see table 5.3), displaying a well reproducible and fairly narrow peak. When adding bPEI solution to DNA prepared in NaCl 0.9% or in Tyrode 2X, respectively, a macroscopically visible precipitation occurred. The aggregates sank to the bottom of the cuvette and were therefore not detected. In water, such precipitation did not occur. To perform the measurements, the apparatus automatically set laser power to values from 0.3 to 1%, indicating much more or larger detectable material in the solutions.

When prepared in NaCl 0.45%, the peak position was shifted to a higher mean value and in Tyrode, the increase of the hydrodynamic diameter was even more pronounced. Furthermore, in the latter dispersant the mean hydrodynamic diameter augmented with time. This led to increasing values for the three samples measured one after each other and thus, a high standard deviation resulted. For bPEI/DNA complexes prepared in NaCl 0.45% or Tyrode, measurements were carried out on the supernatant and macroscopic aggregates are thus not taken into account. For a comparative illustration of the complexes' hydrodynamic diameters in dependence on the dispersant and a representative correlation graph, similar for water, NaCl 0.45% and Tyrode, see figure 5.3.

In water, increasing the plasmid concentration of the bPEI/DNA complexes up to 0.8mg/ml was possible without any precipitation. Compared to the complexes at a DNA concentration of 0.13mg/ml, the mean hydrodynamic diameter was significantly augmented to 231 ± 14.0nm and displayed an increased PDI value of 0.37 ± 0.02.

Table 5.3: Summary of the results obtained by DLS for PEI and PEI/DNA complexes in different dispersants.

	Dispersant	pH	Peak I [nm]	Peak II [nm]	PDI
PEI alone	Water	5.3	20.3 ± 2.1	2.8 ± 1.7	0.26 ± 0.13
	Tyrode	7.7	18.5 ± 3.2	-	0.29 ± 0.07
PEI/DNA	Water	5.5	86.7 ± 2.6	-	0.20 ± 0.01
	NaCl 0.45%	6.5	186 ± 23.3	-	0.30 ± 0.03
	Tyrode	8.1	380 ± 144	-	0.14 ± 0.10

5.2.2 ζ-potential of bPEI and bPEI/DNA complexes in different dispersants

The ζ-potential of bPEI in various media is shown in table 5.4. The values obtained in NaCl 0.45% and Tyrode's solution do not significantly differ from each other, whereas they were importantly decreased when comparing to water. In this latter dispersant, the samples exhibited the best, but still neither very stable nor homogenous data quality.

After complexation of bPEI and DNA in water, we obtained a narrow, precise and reproducible peak. The ζ-potential decreased when increasing the salt concentrations (see table 5.4). Complexes prepared in Tyrode displayed values that were similar to the ones obtained for bPEI alone in the same medium. As seen on figure 5.4, the peak width increased in the following order: water (4.3 ± 0.4mV) < NaCl 0.45% (11.7 ± 0.72mV) < Tyrode (12.8 ± 2.1mV). In general, the phase plot quality was better than for non-complexed bPEI. Again, data were the most homogenous in water, followed by NaCl 0.45% and Tyrode.

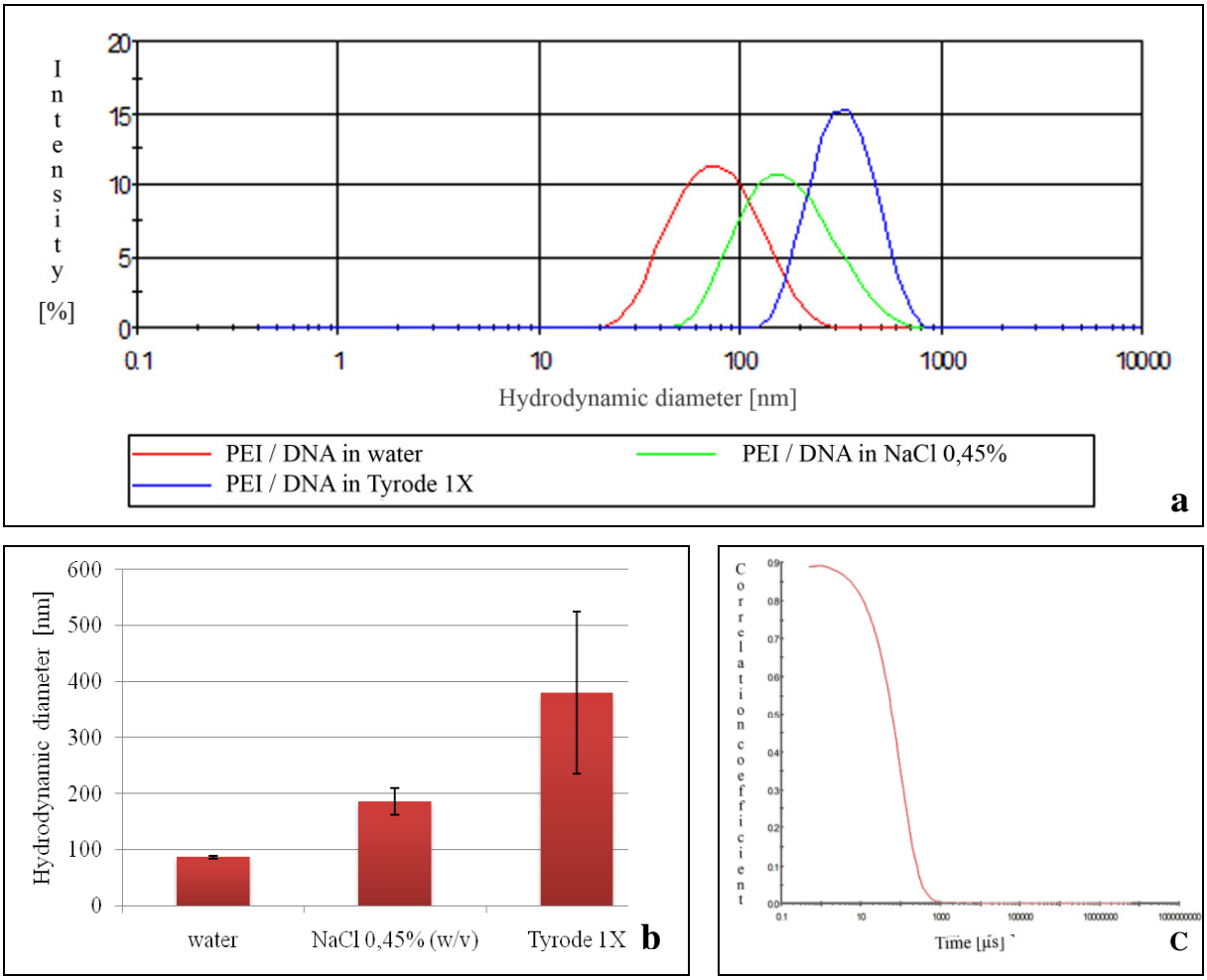

Figure 5.3: Hydrodynamic diameter of bPEI/DNA complexes prepared in different dispersants, measured through DLS: a) Size distribution by intensity, b) Illustration of mean hydrodynamic diameter and standard deviation bars. c) Representative correlation graph for bPEI/DNA complexes, similar for all the three dispersants.

Table 5.4: ζ-potential for PEI and PEI/DNA complexes in different dispersants.

	Dispersant	ζ-potential [mV]
PEI alone	Water	31.4 ± 5.7
	NaCl 0.45%	19.3 ± 6.2
	Tyrode	21.9 ± 7.6
PEI/DNA	Water	47.1 ± 1.2
	NaCl 0.45%	31.7 ± 1.1
	Tyrode	20.9 ± 1.9

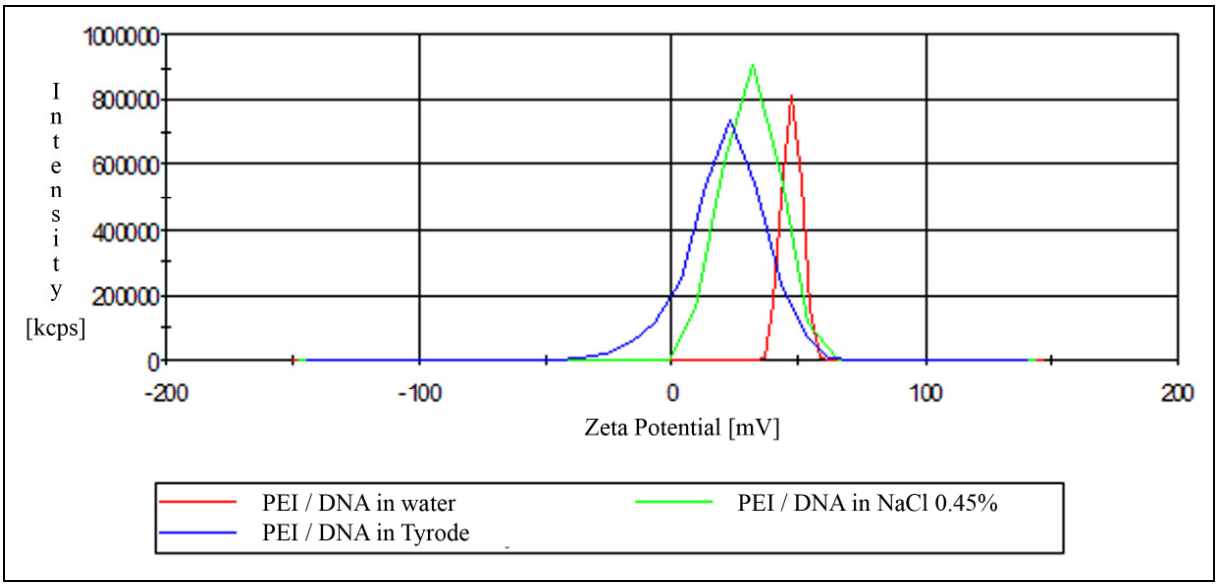

Figure 5.4: ζ-potential distribution of bPEI / DNA complexes in water, NaCl 0.45% and Tyrode's solution.

5.2.3 Size and shape investigations of bPEI/DNA complexes in water by cryo-TEM

To assess the shape of bPEI/DNA complexes formed in water, cryo-TEM experiments were carried out. Relatively small complexes of less than 100nm were detected. The condensates exhibited discrete dense structures (figure 5.5a) as well as folded loops of DNA (figure 5.5b).

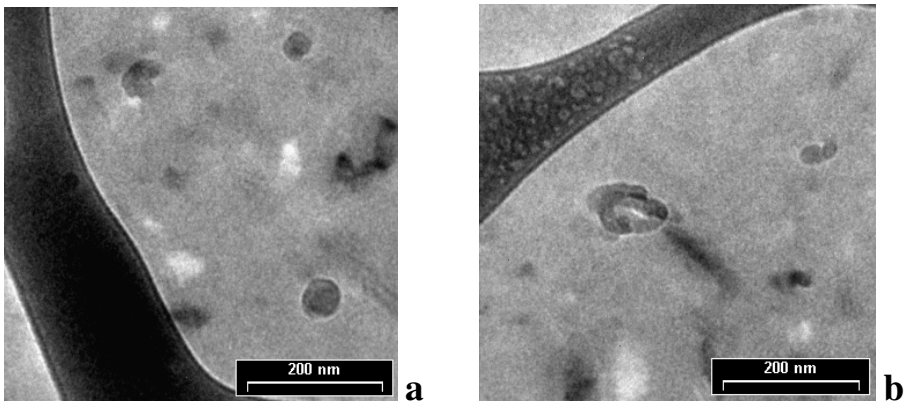

Figure 5.5: cryo-TEM micrographs of bPEI/DNA complexes in water: a) discrete dense DNA condensates and b) folded DNA loop.

5.3 Poloxamine 304/DNA

5.3.1 Size of poloxamine 304 and its formulations in different dispersants

Poloxamine 304 was investigated at 5% (w/v) by DLS measurements in water, NaCl 0.45% and Tyrode. In water and NaCl 0.45%, two populations of different sizes were detected (see table 5.5 and figure 5.6a). When poloxamine 304 was added to Tyrode's solution, the samples

became opalescent. Laser power was diminished from 100% in water and NaCl 0.45% to 1% in Tyrode. When looking at the correlation curves (see figure 5.6c), it is obvious that even larger populations, not represented in the distribution by intensity, were present in the samples.

We obtained two similar peaks for poloxamine 304/DNA systems in water as well as in NaCl 0.45% (see table 5.5 and figure 5.6b). The correlation data support the presence of two populations (see figure 5.6d). The count rates for both dispersants were similar but elevated when compared to 5% of poloxamine 304 alone. In water, it was even augmented by 3.5-fold with reference to DNA itself, whereas the value did not change for NaCl 0.45%. For both media, the association of DNA with poloxamine 304 resulted in an increased PDI when compared to the polymer alone.

When preparing DNA in 2X Tyrode's solution and mixing it with a poloxamine 304 solution at 10% in water, no precipitation occurred. Compared to the PDI value for poloxamine 304 alone, polydispersity decreased after DNA addition. A single, relatively reproducible peak was observed, displaying a larger mean hydrodynamic diameter than obtained for the formulations prepared in water and NaCl 0.45%. Within two of the measurements of one sample, a second peak appeared at about 90nm. Laser power was attenuated from 100% (for the complexes in water and NaCl 0.45%) to 0.3% of the maximum in Tyrode.

Table 5.5: Summary of the results obtained by DLS measurements for poloxamine 304 and poloxamine 304/DNA associations in different dispersants.

	Dispersant	pH	Peak I [nm]	Peak II [nm]	PDI
Poloxamine 304	Water	9.7	2.42 ± 0.08	136 ± 31	0.25 ± 0.08
	NaCl 0.45%	9.5	2.54 ± 0.13	140 ± 41	0.27 ± 0.04
	Tyrode	9.3	1378 ± 382	-	0.48 ± 0.14
Poloxamine 304 / DNA	Water	9.6	2.44 ± 0.03	163 ± 6	0.80 ± 0.03
	NaCl 0.45%	9.7	2.39 ± 0.04	136 ± 25	0.75 ± 0.27
	Tyrode	9.4	553 ± 14	-	0.26 ± 0.01

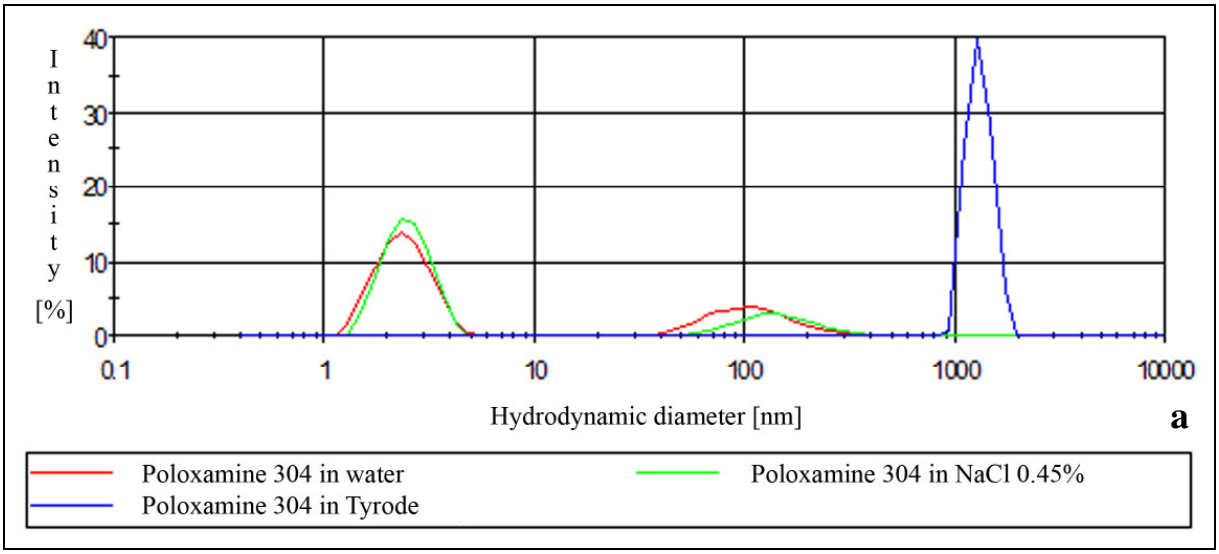

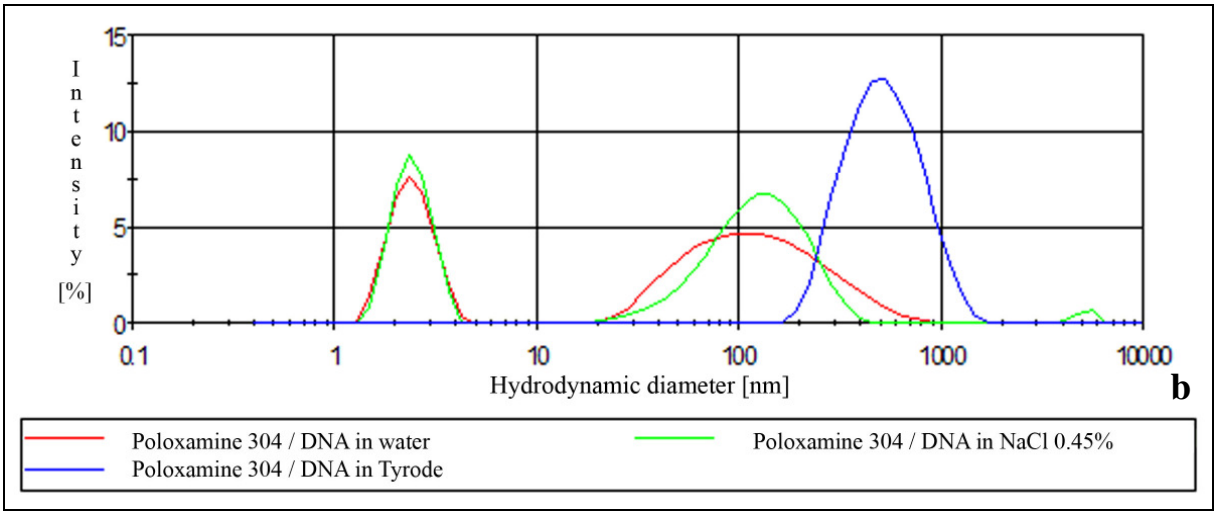

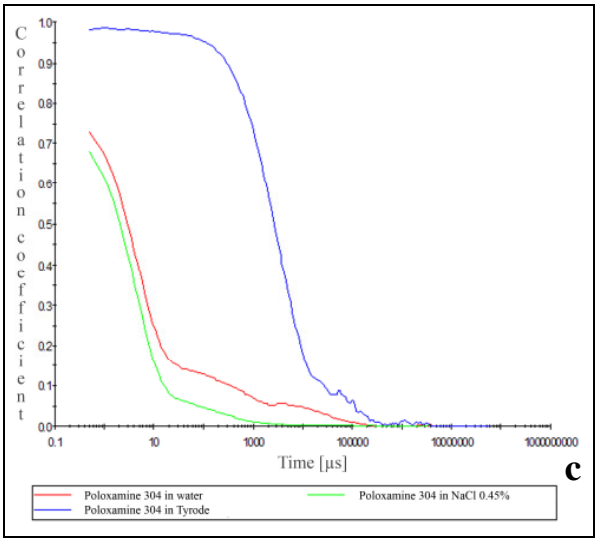

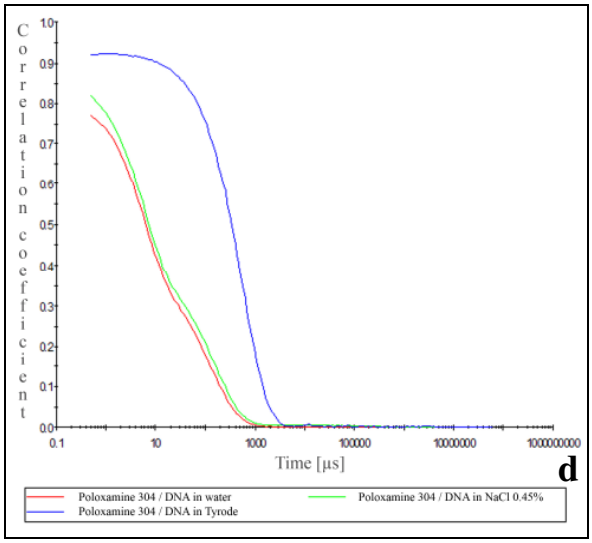

Figure 5.6: Size distribution by intensity of a) poloxamine 304 (5%) and b) poloxamine 304/DNA associations, prepared in different dispersants, measured through DLS. Correlation graphs for c) poloxamine 304 and d) poloxamine 304/DNA associations for all the three dispersants.

When augmenting the plasmid concentration in poloxamine 304/plasmid associations in Tyrode, the hydrodynamic diameters obtained from DLS measurements shifted to higher values (see figure 5.7). A similar tendency occurred for a lower DNA content in the formulations, indicating a minimal hydrodynamic diameter for poloxamine 304/DNA associations prepared with 0.13µg/µl of plasmid.

For 0.5 and 0.8µg/µl of DNA, a second peak which was not very stable and homogenous appeared at a mean average size of 69.4 ± 38.8nm and 93.3 ± 35.2nm, respectively.

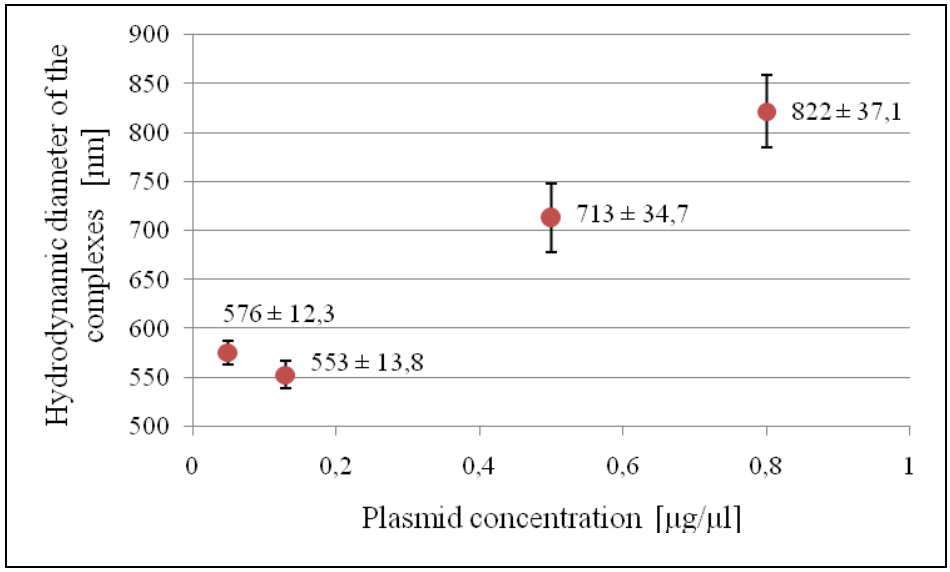

Figure 5.7: Hydrodynamic diameter of poloxamine 304/DNA associations in Tyrode at different DNA concentrations (0.05µg/µl; 0.13µg/µl; 0.5µg/µl; 0.8µg/µl).

5.3.2 ζ-potential of poloxamine 304 and its formulations in different dispersants

In water, the count rate was too low to measure the ζ-potential of poloxamine 304 alone at 5%. Thus, only data in NaCl 0.45% and Tyrode's solution are available and presented on table 5.6. For both dispersants, the phase plot data displayed a low signal to noise ratio.

Associations of poloxamine 304 and DNA prepared in water displayed a clearly negative ζ-potential value which increased for formulations formed in NaCl 0.45%. In contrast, when using Tyrode's solution as dispersant, the ζ- potential was found to decrease again. The ζ-potential of the systems in Tyrode was significantly lower than the one measured for poloxamine 304 alone. For all the three dispersants we obtained neither narrow nor homogenous and stable peaks. Several times, multiple peak profiles were obtained. In general, the phase plot quality was increased when compared to poloxamine 304 alone in Tyrode, but it was still not satisfying. Thereby, in water the data was the most homogenous.

Table 5.6: ζ-potential for poloxamine 304 and poloxamine 304/DNA associations in different dispersants.

	Dispersant	ζ-potential [mV]
Poloxamine 304 alone	Water	-
	NaCl 0.45%	-4.6 ± 2.8
	Tyrode	1.3 ± 1.1
Poloxamine 304 / DNA	Water	-23.4 ± 2.7
	NaCl 0.45%	-11.8 ± 2.2
	Tyrode	-20.9 ± 1.1

5.3.3 Size and shape investigations of poloxamine 304/DNA associations in Tyrode by cryo-TEM

To investigate the shape of poloxamine 304/DNA associations formed in Tyrode's solution, cryo-TEM experiments were carried out. Two different particle populations, displaying various shapes, were found. Spherical condensates of less than 100nm with plane surfaces, are shown on figure 5.8a. Figure 5.8b illustrates a single sphere with a grained or a kind of hairy exterior.

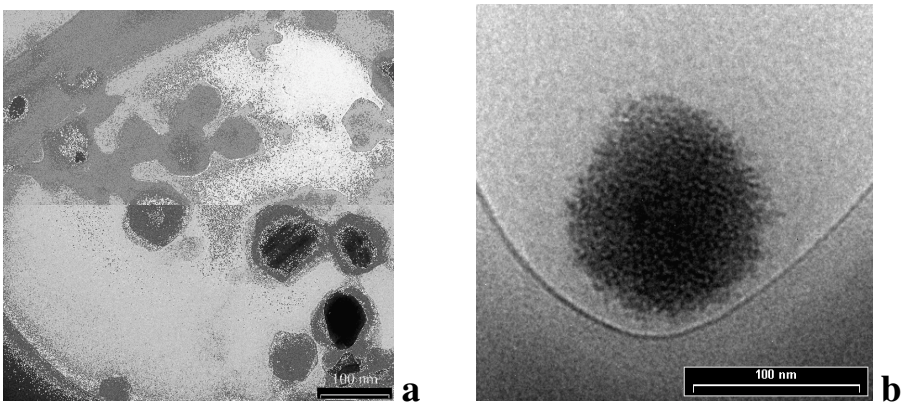

Figure 5.8: cryo-TEM micrographs of Poloxamine 304/DNA associations in Tyrode's solution: a) Spherical condensates with a plane surface. b) Single sphere with grained or hairy exterior.

5.4 PE6400/DNA

5.4.1 Size of PE6400 and PE6400/DNA formulations in different dispersants

As a reference, a solution of 0.05% of the poloxamer PE6400 was investigated by DLS measurements in water and Tyrode's solution. Laser power was automatically set to maximum transmission, when measuring such a strongly diluted sample, but still the count

rate was almost at the lower limit for both dispersants. Similar size distribution profiles with two peaks were obtained for water as well as for Tyrode (figure 5.9a). The first peak of smaller size displayed close but significantly different values for water and Tyrode, whereas a second one displayed a larger hydrodynamic diameter without any significant differences depending on the dispersant. The PDI values were found to be similar as well. Correlation data for both dispersants was of very poor quality and hardly analyzable. Since for water and Tyrode's solution almost the same size intensity profiles were obtained, comparable results are also expected in NaCl 0.45%. The results are summarized in table 5.7.

For the assessment of the associations between plasmid and copolymer, the laser beam was set to maximum power again. In comparison to PE6400 alone, all samples displayed a higher mean count rate that was similar to the one obtained for DNA alone in the same dispersants. The evaluation of PE6400/DNA led to the following results: for all the three dispersants, the data resemble to the ones obtained for DNA alone in water. In water, several times a peak of about 4.9nm was detected that did not appear when measuring DNA alone. It might somehow correspond to the peak at 3.1nm obtained by the investigations of PE6400 alone. For a summary of the results see table 5.7; size distribution graphs for the formulations prepared in the salt containing dispersants are illustrated in figure 5.9b.

Table 5.7: Summary of the results obtained by DLS measurements for PE6400 and PE6400/DNA complexes in different dispersants.

	Dispersant	pH	Peak I [nm]	Peak II [nm]	PDI
PE6400	Water	5.8	3.1 ± 0.6	211 ± 30	0.72 ± 0.19
	Tyrode	8.1	3.7 ± 0.6	231 ± 81	0.67 ± 0.17
PE6400/DNA	Water	5.8	4.9 ± 1.1	- *	0.62 ± 0.15
	NaCl 0.45%	6.7	16.8 ± 2.1	118 ± 9	0.33 ± 0.06
	Tyrode	8.4	22.4 ± 10.2	146 ± 15	0.33 ± 0.04

* As several unstable peaks were obtained, no mean value may be indicated.

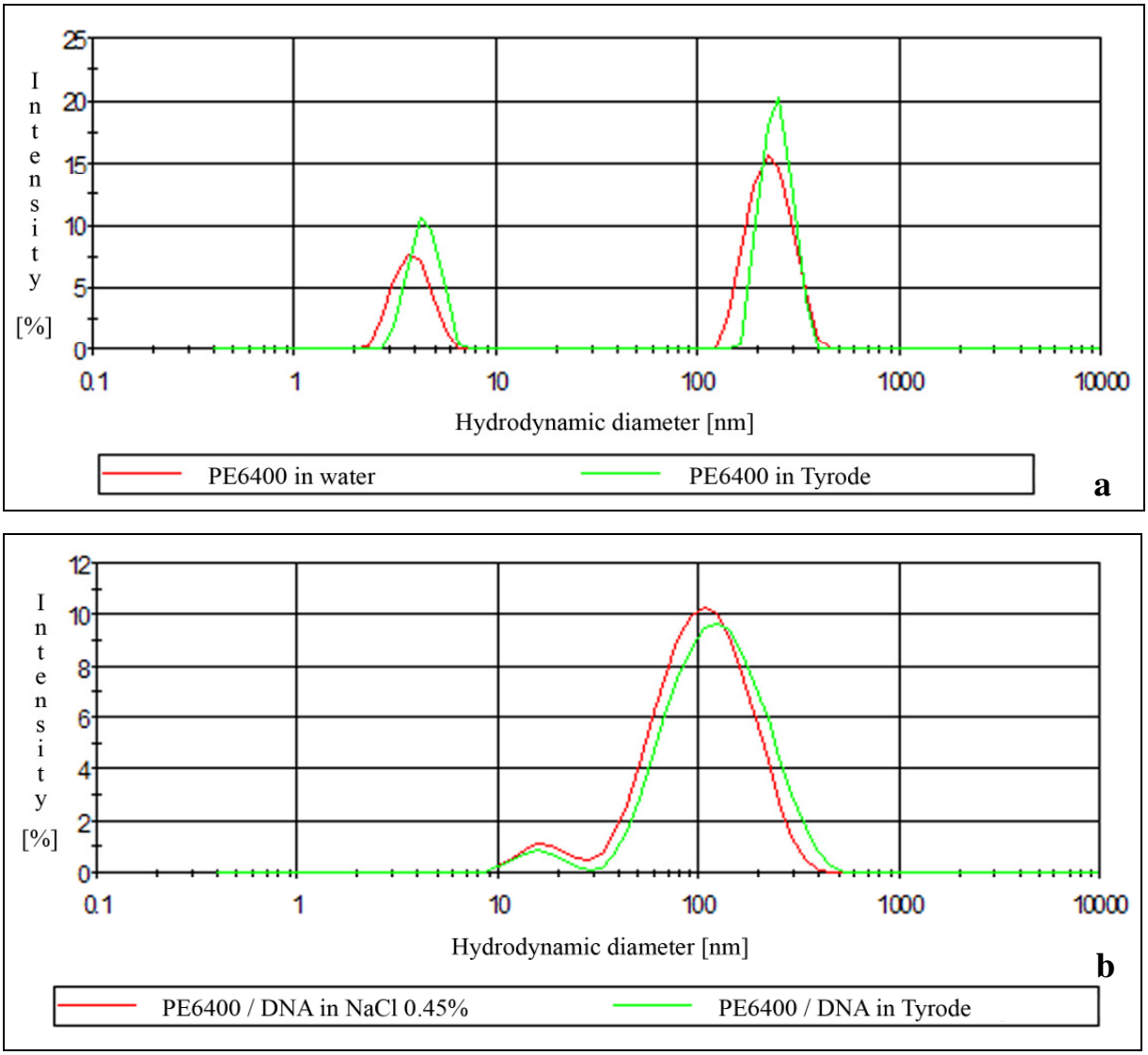

Figure 5.9: Size distribution by intensity of a) PE6400 (0.05%) prepared in water and Tyrode's solution and b) PE6400/DNA systems in NaCl 0.45% or Tyrode, measured through DLS.

For PE6400/DNA formulations in Tyrode's solution, no differences were observed when the DNA concentration was increased up to 0.8µg/µl. Although the attenuation of the laser beam was raised, representing the augmentation of DNA concentration, the DLS profile still resembles to DNA alone in Tyrode (data not shown).

5.4.2 ζ-potential of PE6400 and its formulations in different dispersants

As PE6400 is a non-ionic block copolymer, no ζ-potential measurements could be achieved. No results were obtained either, when trying to determine the ζ-potential of PE6400/DNA associations in water. Thus, only data for the complexes prepared in NaCl 0.45% and in Tyrode's solution are available. For these two dispersants, 100% of the laser beam was used.

The values obviously resemble the data obtained from DNA alone, whereas in Tyrode a less negative potential was detected. The zeta potential was determined as displayed on table 5.8.

Table 5.8: ζ-potential for PE6400/DNA systems in different dispersants.

	Dispersant	ζ-potential [mV]
PE6400/DNA	Water	-
	NaCl 0.45%	-31.8 ± 2.8
	Tyrode	-24.5 ± 4.1

5.4.4 Size and shape investigations of PE6400/DNA formulations in Tyrode by cryo-TEM

PE6400/DNA associations were prepared in Tyrode's solution to examine their shape by cryo-TEM investigations. Spherical structures were obtained, as shown in figure 5.10. The vesicles display varying sizes, ranging from about 10 to 50 nm.

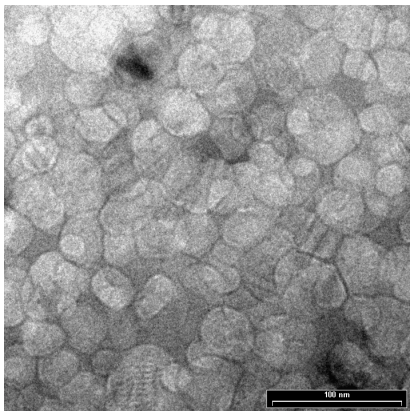

Figure 5.10: cryo-TEM investigation of PE6400/DNA formulations in Tyrode's solution: arrangement of spherical formations of different size, lamellar structures at the bottom image border.

5.5 rM-β-CD/DNA, rM-β-CD/cholesterol/DNA and rM-β-CD/DC-cholesterol/DNA

To examine the rM-β-CD containing formulations' effects for muscular tissue *in vivo*, a toxicological study preceded the present work. rM-β-CD solutions of different concentrations were injected into tibialis anterior and quadriceps muscles of Syrian hamsters. Seven days later the animals were sacrificed with an overdose of anesthetics and the muscles were removed and analyzed. As expected, toxicity increased with CD concentration, displaying severe inflammations and necrosis from 2 to 10% (w/v) of rM-β-CD. Since for 1%, but not

for 0.5%, a local inflammation at the injection site was still observed, we chose to principally examine the latter concentration in our formulations.

5.5.1 Size investigations of rM-β-CD, rM-β-CD/cholesterol and rM-β-CD/DC-cholesterol before and after addition of DNA

Table 5.9: Summary of the results obtained by DLS for rM-β-CD, rM-β-CD/cholesterol, rM-β-CD/DC-cholesterol and their associations with DNA in water and Tyrode.

	Dispersant	pH	Peak I [nm]	Peak II [nm]	Peak III [nm]	PDI
rM-β-CD	Water	6.3	1.76 ± 0.08	-	233 ± 76	0.43 ± 0.10
	Tyrode	8.2	1.95 ± 0.12	-	280 ± 66	0.37 ± 0.10
rM-β-CD / cholesterol *	Water	6.5	1.83 ± 0.03	56.0 ± 10.0	280 ± 37	0.49 ± 0.10
	Tyrode	8.2	2.21 ± 0.05	-	431 ± 57	0.47 ± 0.08
rM-β-CD / DC-cholesterol	Water	6.5	1.89 ± 0.11	-	287 ± 80	0.39 ± 0.15
	Tyrode	8.1	2.16 ± 0.13	-	330 ± 54	0.34 ± 0.07
rM-β-CD / DNA	water §	6.5	1.82 ± 0.10	-	-	0.39 ± 0.22
	Tyrode	8.1	-	25.1 ± 3.1	141 ± 13	0.37 ± 0.09
rM-β-CD / cholesterol / DNA	Water	6.8	1.93 ± 0.17	29.4 ± 9.2	166 ± 17	0.53 ± 0.21
	Tyrode	8.2	-	22.8 ± 7.2	127 ± 16	0.45 ± 0.07
rM-β-CD / DC-cholesterol / DNA	Water	6.7	2.07 ± 0.17	22.9 ± 8.6	174 ± 27	0.61 ± 0.18
	Tyrode	8.0	-	20.2 ± 6.2	163 ± 34	0.48 ± 0.02

If not otherwise noted: [rM-β-CD] = 0.5% (w/v), rM-β-CD/DC-cholesterol = 15:1, rM-β-CD/DC-cholesterol = 15:1, [DNA] = 0.13 µg/µl. * [rM-β-CD] = 1%. § Apart from the monomeres' peak, profile not stable enough to indicate mean diameters.

rM-β-CD itself was examined by DLS measurement at 0.5% (w/v) in water as well as in Tyrode's solution. Solutions of rM-β-CD at 1% (w/v) were diluted to 0.5% to guarantee the same conditions of preparation like later applied for CD association to the plasmid. The size profiles obtained in the two dispersants resembled each other and thus, investigations in NaCl 0.45% were not carried out. For both, maximal laser power was applied automatically, but the mean count rate remained at the lower limit. The most intense peak (peak I) represented in table 5.9 was stable within all samples. In Tyrode, it displayed a significantly larger hydrodynamic diameter than in water. A second peak was also detected (see table 5.9). The hydrodynamic diameters obtained in the two dispersants were not significantly different and the PDI values resembled to each other, as well. For the size distribution by intensity depending on the dispersant, see figure 5.11.

Within the majority of the samples, a further, low intense population of large aggregates appeared at 4500 to 5500nm, whereas it needs to be kept in mind that only particles up to 6000nm may be detected by the apparatus. We tried to eliminate the large structures by filtration through 0.80µm and 0.22µm polyvinylidene fluoride (PVDF) filters as well as through 0.45µm cellulose acetate (CA) membranes. We did neither succeed in removing these large aggregates from the solutions of rM-β-CD in water, nor in Tyrode. For PVDF membranes of 0.22µm, a decrease in the intensity of the smaller aggregates' peak and a significantly increased hydrodynamic diameter of the monomers occurred for both dispersants. Furthermore, the hydrodynamic diameter of the monomers decreased when using CA membranes of 0.45µm. 10min of centrifugation at up to 6000rpm, was not sufficient to achieve a separation of the large structures either.

When preparing a rM-β-CD solution at 1% (w/v), the size distribution profiles did not significantly change (data not shown).

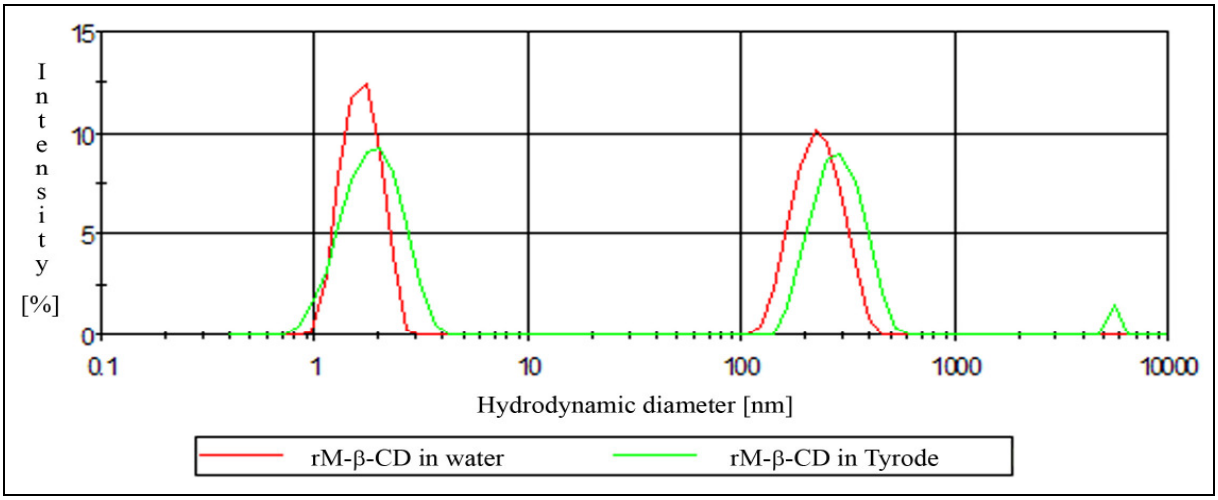

Figure 5.11: Size distribution by intensity of rM-β-CD (0.5%) prepared in water and Tyrode's solution, investigated by DLS measurements.

The complexes between rM-β-CD and cholesterol were prepared by method #2 ([rM-β-CD] = 1%; CD/cholesterol molar ratio = 15:1) and afterwards investigated by DLS. In water, the apparatus detected three populations, as shown on table 5.9. Thereof, the one representing the CD monomers was significantly increased in its hydrodynamic diameter when comparing to rM-β-CD alone. Again, µm-sized aggregates were present. When performing the measurement in Tyrode's solution, we observed only two peaks. Both showed significantly larger hydrodynamic diameters than obtained for the same specimens prepared in water and than rM-β-CD itself in Tyrode's solution. For both dispersants, again full laser power was applied, but as expected, the mean count rate was higher than for 0.5% of rM-β-CD. As the

size distribution profiles strongly resemble the ones obtained for rM-β-CD alone (see figure 5.11), the curves are not shown.

Afterwards, the solutions at 1% rM-β-CD were half diluted with water or Tyrode. Thereby, the samples turned opalescent, suggesting a precipitation of cholesterol that was confirmed by the results of DLS investigations. The PDI increased from 0.49 ± 0.10 to 0.99 ± 0.03 in water and from 0.47 ± 0.12 to 0.96 ± 0.08 in Tyrode's solution. When looking at the correlation graph (see figure 5.12), the presence of large particles is obvious. The noise after 10000µs may be improved by increasing the number of measurements or the run time.

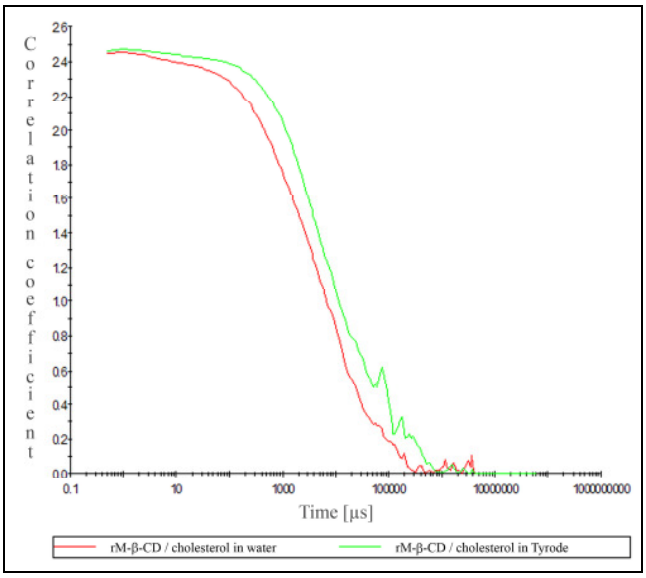

Figure 5.12: Correlations graphs of rM-β-CD/cholesterol ([rM-β-CD] = 0.5%, rM-β-CD/cholesterol = 15:1) associations in water and Tyrode a) before and b) after dilution from [rM-β-CD] = 1% by water or Tyrode.

By direct preparation of rM-β-CD/cholesterol (15:1) complexes at 0.5% of rM-β-CD, a precipitation may be prevented. We obtained results comparable to the ones that were previously described for the non-diluted samples of rM-β-CD(1%)/cholesterol. Complexes containing various rM-β-CD concentrations (0.1%, 2% and 5%) were also tested, whereof all showed the same behavior like the solutions of 0.5% and 1% of rM-β-CD. It was examined, that the monomer's hydrodynamic diameter shifted to higher values with increasing rM-β-CD concentration.

Complexes of rM-β-CD with DC-cholesterol were investigated as well. Automatically, full laser power was set. The size distribution profiles for both dispersants resemble each other, showing two main peaks and a low intense third one of µm-sized aggregates. For both dispersants, the hydrodynamic diameter of the monomers is increased when comparing to the

value obtained for rM-β-CD alone. Furthermore, in Tyrode that diameter is significantly larger than in water. The PDI values hardly differ from each other. Again, the size distribution curves are not shown, since they resemble the ones of rM-β-CD alone in water and Tyrode (see figure 5.11).

Like previously demonstrated for rM-β-CD, it was not possible to separate the µm-sized structures present in the samples by filtration. We just obtained a diminishment in the intensity of the peak displaying the smaller aggregates and a hydrodynamic diameter of the monomer's peak that was shifted to higher values.

Neither variations of the rM-β-CD concentration from 1% to 0.5% nor changes in the rM-β-CD/DC-cholesterol ratio between 15:1 and 60:1 strongly influenced the size distribution profile examined by DLS. We further modified the preparation method from #1 to #2 and again, no significant changes were observed. In contrast to the complexes prepared with non-charged cholesterol, even dilution down to 1/10 (from 5% to 0.5% of rM-β-CD) was possible without any precipitation. A representative example is shown on table 5.9.

Formulations of rM-β-CD and DNA displayed size distribution profiles that resembled the ones obtained for DNA alone in water as well as in Tyrode. In water, the only stable peak was recorded from the rM-β-CD monomer that was less intense than without the presence of DNA in the samples. Like for non-complexed DNA in water no further mean sizes may be indicated. When applying Tyrode as dispersant, the peak that symbolizes monomeric rM-β-CD was no more present in the solutions. For both dispersants, the PDI values were of the same order and again, a low amount of µm-sized particles was detected within the samples. The hydrodynamic diameters of the formulations are displayed on table 5.9.

Furthermore, the stability of the complexes was assessed in a range from 37°C down to 4°C. Thereby, the obtained size distribution profiles did not change importantly.

rM-β-CD, cholesterol and DNA were also associated in water and Tyrode. Thereby, the method of preparation (#1 or #2) did not influence the profiles obtained. All the displayed results were obtained from samples prepared by the latter method.

Although precipitation occurred when diluting the complexes without DNA from 1% of rM-β-CD to 0.5%, such a phenomenon did not happen in the presence of plasmids. In water, the profile was stable enough to indicate three peaks, as displayed on table 5.9. They were accompanied by few µm-sized aggregates. Count rate and attenuation index were alike previously described for rM-β-CD/DNA. Again, the peak for monomeric rM-β-CD was no more present for samples prepared in Tyrode's solution and thus, apart from the µm-sized

structures, two populations remained. The PDI was slightly decreased and displayed a lower standard deviation when using Tyrode as dispersant. For the size distribution profile by intensity, see figure 5.13.

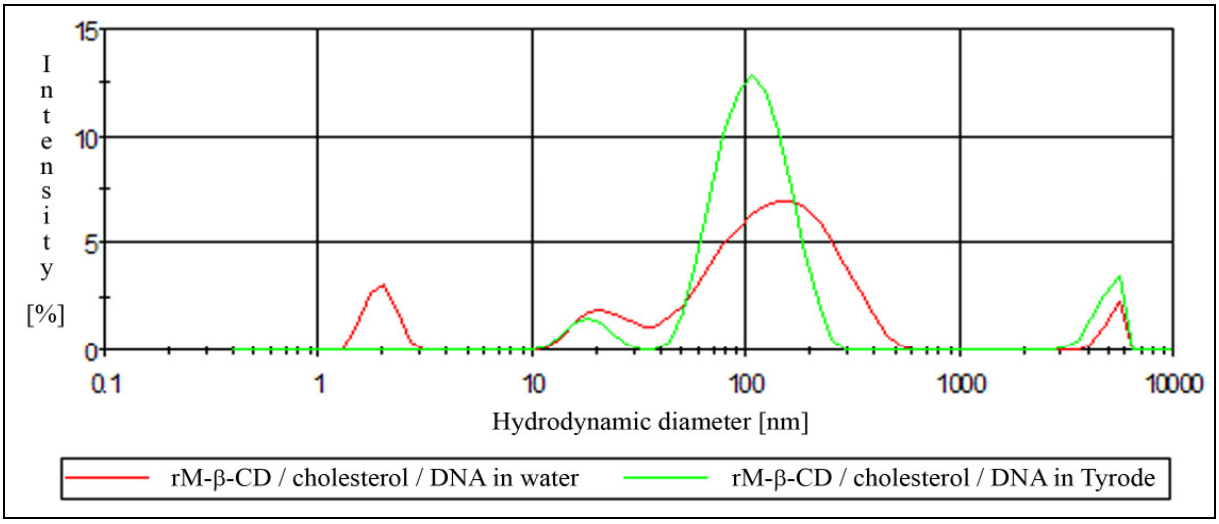

Figure 5.13: Size distribution by intensity of rM-β-CD/cholesterol/DNA ([rM-β-CD] = 0.5%, rM-β-CD/cholesterol = 15:1, [DNA] = 0.13µg/µl) prepared in water and Tyrode's solution investigated by DLS.

Finally, rM-β-CD, DC-cholesterol and DNA were associated and examined ([rM-β-CD] = 0.5%, rM-β-CD/DC-cholesterol = 15:1). As presented on table 5.9, three populations were detected in water. The peak of the rM-β-CD monomers was less intense but the hydrodynamic diameter was increased compared to the solutions without plasmids. As for the same complexes prepared with cholesterol, the size distribution profile generally appeared more stable than the one of uncomplexed DNA or rM-β-CD/DNA in water. Once again, monomeric rM-β-CD was no more found in the samples when using Tyrode as dispersant. Compared to water, the PDI value was decreased in Tyrode's solution.

In both dispersants, the main peaks were accompanied by µm-sized structures. As shown on figure 5.14, the size distribution profile is similar to the one obtained from rM-β-CD/cholesterol/DNA.

As a final aspect, preparing rM-β-CD/cholesterol/DNA and rM-β-CD/DC-cholesterol/DNA complexes in Tyrode at DNA concentration up to 0.8µg/µl, did not significantly change the results. The size distribution profile obtained was similar to the one recorded from the samples at low plasmid concentration. Since more material was present in the samples, laser power was more attenuated (10%). The DLS profile resembled to naked DNA in Tyrode.

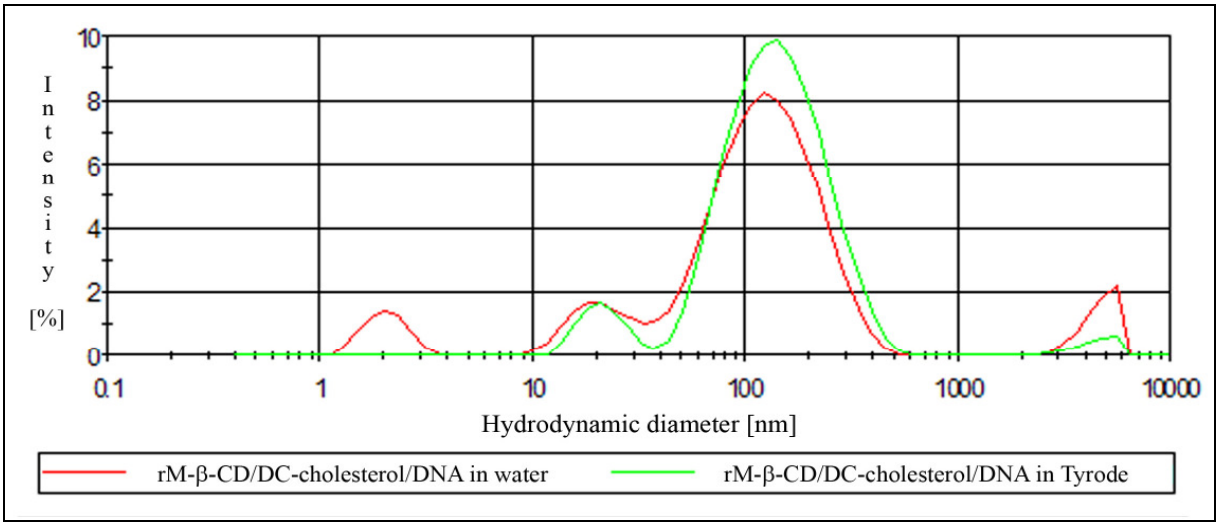

Figure 5.14: Size distribution by intensity of rM-β-CD/DC-cholesterol/DNA ([rM-β-CD] = 0.5%, rM-β-CD: DC-cholesterol = 15:1, [DNA] = 0.13µg/µl) prepared in water and Tyrode, investigated by DLS measurements.

5.5.2 ζ-potential measurement of rM-β-CD/cholesterol/DNA and rM-β-CD/ DC-cholesterol/DNA complexes

Table 5.10: Summary of the results obtained by ζ-potential measurements for rM-β-CD, rM-β-CD/cholesterol, rM-β-CD/DC-cholesterol and their associations with DNA in water and Tyrode.

	Dispersant	ζ-potential [mV]
rM-β-CD	Water	- *
	Tyrode	- *
rM-β-CD / cholesterol	Water	-23.1 ± 5.7
	Tyrode	-9.8 ± 4.4
rM-β-CD / DC-cholesterol	Water	- *
	Tyrode	- *
rM-β-CD / DNA	Water	- *
	Tyrode	- *
rM-β-CD / cholesterol / DNA	Water	- *
	Tyrode	-19.9 ± 5.7
rM-β-CD / DC-cholesterol / DNA	Water	-48.9 ± 2.6
	Tyrode	-27.0 ± 2.6

If not otherwise noted: [rM-β-CD] = 0.5% (w/v), rM-β-CD/cholesterol = 15:1, rM-β-CD/DC-cholesterol = 15:1, [DNA] = 0.13 µg/µl. * Count rate too low to perform the measurements.

No ζ-potential could be recorded with rM-β-CD or rM-β-CD/DC-cholesterol complexes, neither in water nor in Tyrode, but the apparatus succeeded in calculating a ζ-potential for rM-β-CD/cholesterol. As displayed on table 5.10, a strongly negative value was obtained in water, whereas for Tyrode's solution, the ζ-potential was found to be less negative.

When having tried to evaluate the association between rM-β-CD and DNA in both dispersants and between rM-β-CD, cholesterol and DNA in water, the count rate was not sufficient to perform the measurements. Thus, for the latter formulation only values for Tyrode's solution are available (see table 5.10). The ζ-potential displayed by the samples is increased when compared to naked DNA, but still negative.

Formulations associating rM-β-CD, DNA and single positively charged DC-cholesterol were found to exhibit a ζ-potential that was as negative as -50mV in water. The intensity of the peak was much lower than for the formulations prepared in Tyrode's solution. For the latter dispersant we obtained values that were similar to the ones for naked DNA in Tyrode. The ζ-potential distribution graphs for rM-β-CD/cholesterol/DNA in Tyrode and rM-β-CD/DC-cholesterol/DNA in both dispersants are given on figure 5.15.

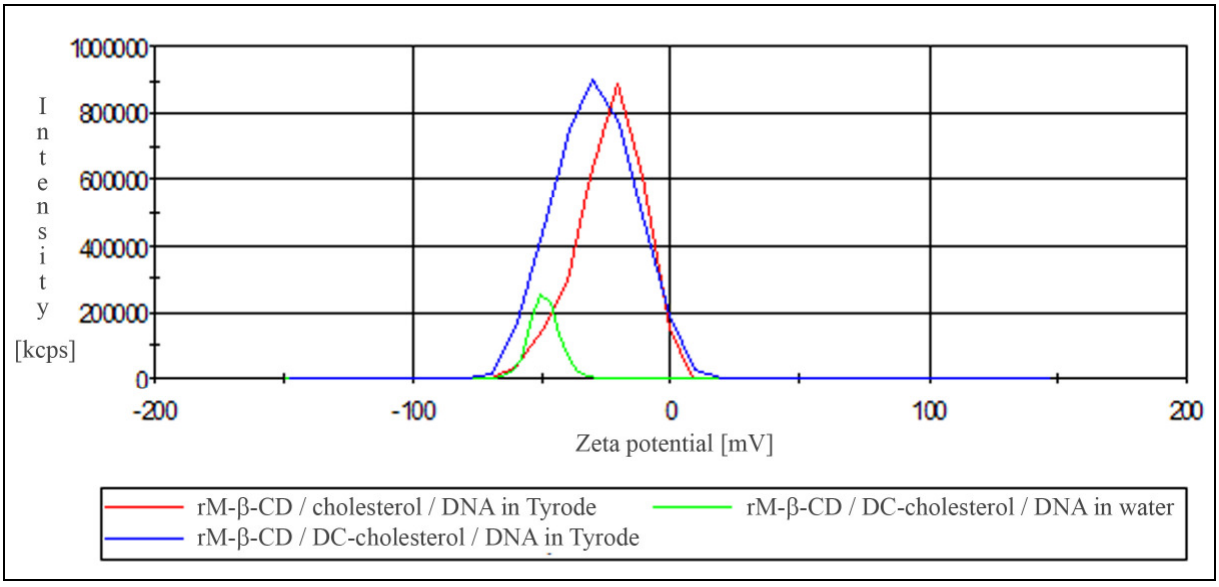

Figure 5.15: ζ-potential distribution of rM-β-CD/cholesterol/DNA in Tyrode and rM-β-CD/DC-cholesterol/DNA in water and Tyrode.

6 Discussion

We investigated the size distribution profiles of various plasmid/vector associations recorded through Dynamic Light Scattering to characterize and evaluate these gene delivery systems. Depending on the different physicochemical properties of several non-viral carriers, advantages as well as limits of the technique were studied. Polycationic bPEI, monocationic poloxamine 304 and non-charged PE6400 were chosen as polymeric vector systems and single positively charged DC-cholesterol or uncharged cholesterol associated to rM-β-CD were evaluated as lipidic carriers.

The technique of DLS offers many advantages. In general, nanoscopic particles as well as µm-sized ones may be investigated, whereas the Zetasizer Nano ZS is applicable from 0.6nm to 6µm. Structures of less than 2nm and associations of several µm in their hydrodynamic diameter were detected, making that wide size range valuable for our work. pCMVβGal itself shows a size well fitting for DLS experiments. Except for some large aggregates present in the rM-β-CD containing formulations, the carrier-associated structures to be measured within the different samples were of suitable size, either.
Due to the feature of automatically or manual laser power regulation, diluted samples as well as highly concentrated ones may be measured. The plasmid concentration used for our investigations was chosen, since it needed to be applicable for *in vivo* investigations carried out besides the physicochemical characterization reported within this work (data not shown). As 150µl of each formulation were injected at once and 20µg of DNA were set as initial plasmid amount per injection, all the samples were prepared at a plasmid concentration of 0.13µg/µl. Especially for the rM-β-CD and PE6400 containing systems we therefore had to work at the minimum concentration detectable by the device. Anyway, analyzable profiles were obtained, since the apparatus compensates low concentration by performing a greater number of measurements on one sample to statistically augment the reliability of the results.
Further attention shall be paid to the high precision of the technique that was already useful when just measuring pCMVβGal itself: we detected variations between the size profiles obtained from the plasmid alone, purified by two different purification kits, although there were no differences visible from UV spectrophotometry and gel electrophoresis investigations. Thus, we may recommend additionally testing of DNA after its purification by DLS to verify its actual conformation.

Through DLS, the hydrodynamic diameters of the investigated DNA/vector associations are obtained, whereas different types of data may be consulted as results and quality criteria. Although almost all our samples, whatever they were composed of, showed a relatively high polydispersity index and more than just one size population, suitable data could be obtained. We did not rely onto the Z-average, as that parameter is mainly applicable for monodisperse samples. Instead, the size distribution profiles and the hydrodynamic diameters of each single peak were interpreted and evaluated.

When comparing the profiles of the plasmid/vector associations to the ones obtained from DNA or the non-viral carrier alone, conclusions about the existence of interactions may be drawn. Thereby, the strength of the involved forces between the formed associations is assessable from the stability of the size peaks' position and shape during the measurement of one sample. Reproducibility needs to be taken into account as well.

To additionally prove the data, it is advisable to consult the correlograms which represent the raw material recorded by the device prior to any transformation by arithmetic operations. For small, rapidly moving particles, the correlation curve exhibits a fast decay rate, whereas for large particles the graph's decay occurs on a much longer time scale, indicating slower diffusion rates. Thus, the information drawn from such curves are strongly associated to the ones obtained from the size distribution profiles.

For bPEI/DNA and poloxamine 304/DNA, obviously different size distribution profiles were obtained when comparing them to the ones recorded for the polymer or DNA alone. Thus, relatively strong interactions that are well detectable by the technique may be indicated. However, the information that could be drawn from the investigation of the PE6400 and rM-β-CD containing formulations were not that clear. The hydrodynamic diameters of the non-viral carriers are of the same size range as DNA alone and the results obtained for the plasmid/vector associations strongly resembled the ones obtained for the plasmid, either. That behavior makes it impossible to conclude about the existence of interactions and restricts the use of DLS for our concerns.

To gain further information, we investigated the plasmid/vector associations in several dispersants. The modifications within the samples are easily compensated through adaptations of the devices' automatic calculation of the hydrodynamic diameter. Depending on the dispersant, differences in the size distribution profiles and the general comportment of the associated structures could be pointed out.

We chose water as a non-ionic medium, NaCl 0.45% as an ionic solution of monocations and monoanions, and Tyrode, a physiological aqueous electrolyte additionally containing divalent

cations. There is no dispersant that may generally be considered as the optimal one, as that criterion depends on the presence of a gene delivery vector as well as on the vector type used to associate the plasmid.

For DNA alone, an augmentation in ionic strength of the medium slightly stabilizes and homogenizes the size distribution profile, since homogeneity increased from water over NaCl 0,45% to Tyrode's solutions (to be seen as a decrease in the PDI value). That might be due to the overall ion concentration as well as to the presence of double positively charged ions. To further evaluate this hypothesis, another dispersant might be investigated, displaying the ionic force of Tyrode's solution but resulting from monocations only.

When DNA was attendant in the PE6400 or rM-β-CD containing formulations, similar results were obtained. However, for NaCl and Tyrode the peak of only a few nm, appearing for the vectors alone, was not detected anymore. In the presence of Tyrode, the mean count rate for these plasmid/vector associations was increased by up to 4-fold when compared to water. Thus, that peak might be masked, since its intensity is diminished relatively in comparison to the plasmid. As the profile of DNA underlay no changes, any interaction potential may be supposed. Another approach assumes PE6400 and the CDs to be arranged around the plasmid in Tyrode and thus, to be no more visible for the device as monomers. When following that assumption, especially in the ionic media interactions are considered to exist. The information obtained from DLS does not suffice to settle that question.

For the CD-associated systems, the peaks generally displayed larger hydrodynamic diameters in Tyrode's solution. Since the device does not measure the actual size of the systems, such differences might be due to an influence of the divalent cations onto the hydrodynamic conditions within the formulations. That may be proved as previously described for DNA alone.

Variation of the medium most clearly affects the characteristics of the formulations containing poloxamine 304 or bPEI as non-viral carriers. For poloxamine 304/DNA, a strong influence of divalent cations is emphasized, as the size distribution profiles are similar for water and NaCl 0.45%, but clearly different for Tyrode's solution. In water and NaCl, the smaller-sized of the two peaks clearly results from poloxamine 304, whereas the larger one resembles the major peak of naked DNA as well as the larger population of poloxamine 304 alone. Thus, we have to wonder if any complexation took place. Applying DLS investigations could not satisfyingly answer that question for these two dispersants, since an overlay between the peaks of the plasmids and of poloxamine 304 may exist.

However, in Tyrode's solution, the size distribution profile differs completely. As only one peak was detected and since the PDI value was strongly decreased, the copolymer is indicated to better-associate to the DNA molecules. At a physiological pH, poloxamine 304 exhibits a single positive charge [25]. Thus, the divalent cations present in Tyrode might act as a third complexating partner and help the copolymer associating to the plasmid.

Although some answers still lack, when interpreting all the results obtained for the different media, DLS gave insightful information concerning poloxamine 304/plasmid associations.

For bPEI, we noticed the formation of relatively small complexes in water, whose hydrodynamic diameter is consistent with the results obtained by *Tang and Szoka* [76]. The complexes' hydrodynamic diameter is smaller than for the plasmid alone, indicating successful complexation and compaction of pCMVβGal. bPEI efficiently complexes plasmid which results from electrostatic attraction forces between the negatively charged DNA molecules and polycationic bPEI, hampering dynamic movement within the samples. The hydrodynamic diameter of the complexes is to be seen advantageously for gene delivery, since the large size of DNA is one of the difficulties to overcome in gene therapy. Otherwise, the strong complexation could be a limiting factor as well, since the plasmid has to be released from the vector before its transcription into mRNA and its final expression. In contrast to the other systems, water was the only dispersant allowing bPEI/DNA complexes to display stable and homogeneous profiles. The presence of ions led to an important precipitation of the plasmid and to an increased hydrodynamic diameter of the polyplexes remaining in solution.

We also investigated the influence of various DNA concentrations onto the systems. When working at the lower concentration limit detectable by the device, further dilution of the samples is not possible. In contrast, augmenting the plasmid concentration causes no problems. For the carriers that were already suggested to undergo little or no interactions with pCMVβGal (PE6400, rM-β-CD, rM-β-CD/cholesterol and rM-β-CD/DC-cholesterol), little differences in the size distribution profiles were detected when increasing DNA quantity within the samples. The influence of the plasmid concentration is more obvious when applying bPEI and poloxamine 304. For both, augmenting the DNA concentration leads to an increased hydrodynamic diameter, whereas for poloxamine 304, the same effect further occurred when decreasing the plasmid amounts. Concerning low DNA concentrations within the poloxamine 304 containing samples, the results of *Pitard et al.* [29] are consistent with our findings.

We examined, whether the increased diameter of the formulations containing higher DNA quantities results from a relative decrease in Tyrode's salt concentration: apart from the reappearance of the poloxamine 304 peak at approximately 2.4nm and a general decrease in homogeneity, down to a Tyrode's salt concentration of 0.5X no size shifts were detected. From our investigations, a minimum hydrodynamic size is found for 0.13µg/µl of pCMVβGal. However, to obtain a precise curve progression displaying the hydrodynamic size depending on the plasmid concentration, further samples of different quantitative compositions should be measured.

As a further aspect, the reported observations concerning the effects after dilution of the rM-β-CD/cholesterol samples shall be mentioned. In comparison to the DC-cholesterol containing formulations, the samples show a different comportment when being diluted and thus, different phase solubility behaviors are suggested. Depending on the lipid, varying Higuchi diagrams are expected and consequently, better comprehension of those systems should be achieved by carrying out phase solubility experiments.

To overall consider our examinations, it needs to be kept in mind that the device does not display the actual size of the particles, but their hydrodynamic diameter. That value corresponds to the diameter of the sphere, diffusing at the same speed as the sample being measured.

Moreover, the shape of the systems under evaluation cannot be determined through the technique, making it necessary to additionally perform morphological analysis as cryo-TEM, for example.

From such investigations we gained further information, broadening our idea of the plasmid/vector associations. As already established through DLS measurements, bPEI/DNA complexes formed in water were found to be well-compacted and smaller than 100nm. The detection of discrete dense structures and folded loops of DNA conforms to prior investigations [77]. For poloxamine 304, the results are consistent with those obtained by DLS, as well. Both techniques introduced the existence of two differently sized populations, but only cryo-TEM measurements allowed characterizing the particle's surfaces, that varied for the two populations. In contrast, PE6400/plasmid associations display a more complex behavior and the structures observed through cryo-TEM investigations might be too dynamic to be evaluated with DLS. Until now, pCMVβGal alone was not analyzed through cryo-TEM. It is of particular interest to determine the influence of the medium onto the plasmid's morphology alone, for the results may serve as a reference for the plasmid/vector associations.

Yet, micrographs of the CD containing formulations have not been recorded, either. Such investigations will obtain high priority in following experiments.

When working with charged material, the surface potential of the structures importantly influences gene transfer's efficiency and consequently, appropriate investigations are of particular interest. The Nernst potential itself cannot be examined, but as any relation between charged particles present in the same medium depends on the ζ-potential, we referred to that value.

As expected, for pCMVβGal the ζ-potential is negative, since it displays a negatively charged phosphate backbone and the values become highly positive when the plasmid was complexed by an excess of bPEI. In accordance to the DLS results for bPEI/DNA, we obtained the highest data quality in water.

For poloxamine 304/DNA associations, the ζ-potential was generally similar to the one of pure DNA, whereas it was much lower than for poloxamine 304 alone. These results suggest the presence of pCMVβGal at the surface of the particles when prepared in Tyrode. In water and NaCl, only very weak interactions may exist between poloxamine 304 and DNA, leading to a more complex behavior of those compounds.

Measurements of the ζ-potential of PE6400/DNA associations confirmed the absence (or weakness) of complexation between the poloxamer and the DNA: the values obtained for both dispersants evaluated were strongly negative and similar to those of DNA alone.

Since rM-β-CD does not display any charge, it was not surprising that we did neither in water nor in Tyrode's solution succeed in determining a ζ-potential for the samples. For rM-β-CD/DC-cholesterol no ζ-potential could be measured, either. Unexpectedly, the apparatus succeeded in calculating a ζ-potential for the rM-β-CD/cholesterol samples, although both molecules do not display any charge. To explain that comportment, further examinations need to be carried out.

7 Conclusion

DLS is a powerful technique that may be generally seen as useful in the characterization of interactions between plasmid and the investigated gene delivery vectors. Thereby, changes in the size distribution profile indicate interactions between the two components. From a small volume of little material concentration lots of information may be obtained, whereas the utility of the measurements to characterize the formulations depends on the carriers used to associate DNA.

Especially for the vectors exhibiting electrostatic interactions with DNA, the method accurately describes the samples in various media and concentrations. For bPEI as well as for poloxamine 304 as complexation partners for pCMVβGal, an interaction potential was clearly visible from the resulting size distribution curves. We further succeeded in demonstrating, whether non-ionic or ionic dispersants should be preferred.

In contrast, DLS does not display an ideal technique to investigate the comportment of DNA and vectors that are expected to undergo more dynamic interactions with the plasmid. The size distribution profiles of the PE6400 and rM-β-CD containing formulations strongly resembled the ones obtained for DNA alone. We well figured out the self-association behavior of the applied CDs, but with the help of DLS as sole technique, the actual existence of interactions between the plasmid and its non-ionic carriers cannot be clearly affirmed.

However, DLS measurement may be used as a screening method to rapidly estimate the characteristics of the DNA/vector complexes, but anyway, a comprehensive study of the systems should comprise additional methods of evaluation.

Bibliography

[1] Lechardeur D, Lukacs GL; Intracellular barriers to non-viral gene transfer. Curr Gene Ther; 2002; 2: 183-194.

[2] Robbins PD, Ghivizzani SC; Viral vectors for gene therapy. Pharmacol Ther; 1998; 80: 35-47.

[3] Uchida M, Natsume H, Kishino T, Seki T, Ogihara M, Juni K, Kimura M, Morimoto Y; Immunization by particle bombardment of antigen-loaded poly-(dl-lactide-co-glycolide) microspheres in mice. Vaccine; 2006; 24: 2120-2130.

[4] Mir LM, Bureau MF, Gehl J, Rangara R, Rouy D, Caillaud JM, Delaere P, Branellec D, Schwartz B, Scherman D; High-efficiency gene transfer into skeletal muscle mediated by electric pulses. Proceedings of the National Academy of Sciences of the United States of America; 1999; 96: 4262-4267.

[5] Neumann E, Schaefer-Ridder M, Wang Y, Hofschneider P; Gene transfer into mouse lyoma cells by electroporation in high electric fields. The EMBO Joumal 1982; 1: 841-845.

[6] Luo D, Saltzman WM; Synthetic DNA delivery systems. Nature biotechnology; 2000; 18: 33-37.

[7] Cross D, Burmester JK; Gene therapy for cancer treatment: past, present and future. Clin Med Res; 2006; 4: 218-227.

[8] Han ZQ, Assenberg M, Liu BL, Wang YB, Simpson G, Thomas S, Coffin RS; Development of a second-generation oncolytic Herpes simplex virus expressing TNFalpha for cancer therapy. The journal of gene medicine; 2007; 9: 99-106.

[9] White RE, Wade-Martins R, James MR; Infectious delivery of 120-kilobase genomic DNA by an epstein-barr virus amplicon vector. Mol Ther; 2002; 5: 427-435.

[10] Hibbitt OC, Wade-Martins R; Delivery of large genomic DNA inserts >100 kb using HSV-1 amplicons. Curr Gene Ther; 2006; 6: 325-336.

[11] Godbey WT, Wu KK, Mikos AG; Poly(ethylenimine) and its role in gene delivery. J Control Release; 1999; 60: 149-160.

[12] Godbey WT, Wu KK, Mikos AG; Poly(ethylenimine)-mediated gene delivery affects endothelial cell function and viability. Biomaterials; 2001; 22: 471-480.

[13] Wightman L, Kircheis R, Rossler V, Carotta S, Ruzicka R, Kursa M, Wagner E; Different behavior of branched and linear polyethylenimine for gene delivery in vitro and in vivo. The journal of gene medicine; 2001; 3: 362-372.

[14] Godbey WT, Wu KK, Mikos AG; Size matters: molecular weight affects the efficiency of poly(ethylenimine) as a gene delivery vehicle. J Biomed Mater Res; 1999; 45: 268-275.

[15] Boussif O, Lezoualc'h F, Zanta MA, Mergny MD, Scherman D, Demeneix B, Behr JP; A versatile vector for gene and oligonucleotide transfer into cells in culture and in vivo: polyethylenimine. Proceedings of the National Academy of Sciences of the United States of America; 1995; 92: 7297-7301.

[16] Lungwitz U, Breunig M, Blunk T, Gopferich A; Polyethylenimine-based non-viral gene delivery systems. Eur J Pharm Biopharm; 2005; 60: 247-266.

[17] Remy JS, Kichler A, Mordvinov V, Schuber F, Behr JP; Targeted gene transfer into hepatoma cells with lipopolyamine-condensed DNA particles presenting galactose ligands: a stage toward artificial viruses. Proceedings of the National Academy of Sciences of the United States of America; 1995; 92: 1744-1748.

[18] Godbey WT, Wu KK, Mikos AG; Tracking the intracellular path of poly(ethylenimine)/DNA complexes for gene delivery. Proceedings of the National Academy of Sciences of the United States of America; 1999; 96: 5177-5181.

[19] Behr JP; Gene transfer with synthetic cationic amphiphiles: prospects for gene therapy. Bioconjug Chem; 1994; 5: 382-389.

[20] Helander IM, Alakomi HL, Latva-Kala K, Koski P; Polyethyleneimine is an effective permeabilizer of gram-negative bacteria. Microbiology; 1997; 143: 3193-3199.

[21] Boeckle S, von Gersdorff K, van der Piepen S, Culmsee C, Wagner E, Ogris M; Purification of polyethylenimine polyplexes highlights the role of free polycations in gene transfer. The journal of gene medicine; 2004; 6: 1102-1111.

[22] Gharwan H, Wightman L, Kircheis R, Wagner E, Zatloukal K; Nonviral gene transfer into fetal mouse livers (a comparison between the cationic polymer PEI and naked DNA). Gene therapy; 2003; 10: 810-817.

[23] Roques C, Salmon A, Fiszman MY, Fattal E, Fromes Y; Intrapericardial administration of novel DNA formulations based on thermosensitive Poloxamer 407 gel. International journal of pharmaceutics; 2007; 331: 220-223.

[24] Moghimi SM, Hunter AC; Poloxamers and poloxamines in nanoparticle engineering and experimental medicine. Trends Biotechnol; 2000; 18: 412-420.

[25] Armstrong JK, Chowdhry BZ, Snowden MJ, Dong J, Leharne SA; The effect of pH and concentration upon aggregation transitions in aqueous solutions of poloxamine T701. International journal of pharmaceutics; 2001; 229: 57-66.

[26] Jones M, Leroux J; Polymeric micelles - a new generation of colloidal drug carriers. Eur J Pharm Biopharm; 1999; 48: 101-111.

[27] Alvarez-Lorenzo C, Gonzalez-Lopez J, Fernandez-Tarrio M, Sandez-Macho I, Concheiro A; Tetronic micellization, gelation and drug solubilization: Influence of pH and ionic strength. Eur J Pharm Biopharm; 2006.

[28] Lemieux P, Guerin N, Paradis G, Proulx R, Chistyakova L, Kabanov A, Alakhov V; A combination of poloxamers increases gene expression of plasmid DNA in skeletal muscle. Gene therapy; 2000; 7: 986-991.

[29] Pitard B, Bello-Roufai M, Lambert O, Richard P, Desigaux L, Fernandes S, Lanctin C, Pollard H, Zeghal M, Rescan PY, Escande D; Negatively charged self-assembling DNA/poloxamine nanospheres for in vivo gene transfer. Nucleic acids research; 2004; 32: e159.

[30] Storm G, Belliot S, Daemen T, Lasic D; Surface modification of nanoparticles to oppose uptake by the mononuclear phagocyte system. Adv Drug Deliv Rev; 1995; 17: 31-48.

[31] Csaba N, Caamano P, Sanchez A, Dominguez F, Alonso MJ; PLGA:poloxamer and PLGA:poloxamine blend nanoparticles: new carriers for gene delivery. Biomacromolecules; 2005; 6: 271-278.

[32] Kabanov AV, Batrakova EV, Alakhov VY; Pluronic block copolymers as novel polymer therapeutics for drug and gene delivery. J Control Release; 2002; 82: 189-212.

[33] Pitard B, Pollard H, Agbulut O, Lambert O, Vilquin JT, Cherel Y, Abadie J, Samuel JL, Rigaud JL, Menoret S, Anegon I, Escande D; A nonionic amphiphile agent promotes gene delivery in vivo to skeletal and cardiac muscles. Hum Gene Ther; 2002; 13: 1767-1775.

[34] Richard P, Pollard H, Lanctin C, Bello-Roufai M, Desigaux L, Escande D, Pitard B; Inducible production of erythropoietin using intramuscular injection of block copolymer/DNA formulation. The journal of gene medicine; 2005; 7: 80-86.

[35] Kabanov AV, Batrakova EV, Alakhov VY; Pluronic block copolymers for overcoming drug resistance in cancer. Adv Drug Deliv Rev; 2002; 54: 759-779.

[36] Alakhov V, Klinski E, Li S, Pietrzynsik G, Venne A, Batrakova E, Bronitch T, Kabanov A; Block copolymer-based formulation of doxorubicin. From cell screen to clinical trials. Colloids and Surfaces B: Biointerfaces; 1999; 16: 113-134.

[37] Hashida M, Kawakami S, Yamashita F; Lipid carrier systems for targeted drug and gene delivery. Chem Pharm Bull (Tokyo); 2005; 53: 871-880.

[38] Li S, Ma Z; Nonviral gene therapy. Curr Gene Ther; 2001; 1: 201-226.

[39] Felgner PL, Gadek TR, Holm M, Roman R, Chan HW, Wenz M, Northrop JP, Ringold GM, Danielsen M; Lipofection: a highly efficient, lipid-mediated DNA-transfection procedure. Proceedings of the National Academy of Sciences of the United States of America; 1987; 84: 7413-7417.

[40] Sternberg B, Sorgi FL, Huang L; New structures in complex formation between DNA and cationic liposomes visualized by freeze-fracture electron microscopy. FEBS letters; 1994; 356: 361-366.

[41] Lv H, Zhang S, Wang B, Cui S, Yan J; Toxicity of cationic lipids and cationic polymers in gene delivery. J Control Release; 2006; 114: 100-109.

[42] Lappalainen K, Jaaskelainen I, Syrjanen K, Urtti A, Syrjanen S; Comparison of cell proliferation and toxicity assays using two cationic liposomes. Pharmaceutical research; 1994; 11: 1127-1131.

[43] Castanho MA, Brown W, Prieto MJ; Rod-like cholesterol micelles in aqueous solution studied using polarized and depolarized dynamic light scattering. Biophysical journal; 1992; 63: 1455-1461.

[44] Köster F, Finas D, Schulz C, Hauser C, Diedrich K, Felberbaum R; Additive effect of steroids and cholesterol on the liposomal transfection of the breast cancer cell line T-47D. International journal of molecular medicine; 2004; 14: 769-772.

[45] Templeton NS, Lasic DD, Frederik PM, Strey HH, Roberts DD, Pavlakis GN; Improved DNA: liposome complexes for increased systemic delivery and gene expression. Nature biotechnology; 1997; 15: 647-652.

[46] Liu Y, Mounkes LC, Liggitt HD, Brown CS, Solodin I, Heath TD, Debs RJ; Factors influencing the efficiency of cationic liposome-mediated intravenous gene delivery. Nature biotechnology; 1997; 15: 167-173.

[47] Lawrencia C, Mahendran R, Esuvaranathan K; Transfection of urothelial cells using methyl-beta-cyclodextrin solubilized cholesterol and Dotap. Gene therapy; 2001; 8: 760-768.

[48] Davies M, ME. B; Cyclodextrin based pharmaceutics: past, present and future. Nat Rev Drug Discov; 2004; 3: 1023-1035.

[49] Szejtli J; Introduction and General Overview of Cyclodextrin Chemistry. Chem Rev; 1998; 98: 1743-1754.

[50] Dass CR; Vehicles for oligonucleotide delivery to tumours. J Pharm Pharmacol; 2002; 54: 3-27.

[51] Challa R, Ahuja A, Ali J, Khar RK; Cyclodextrins in drug delivery: an updated review. AAPS PharmSciTech; 2005; 6: E329-357.

[52] Davis ME, E. BM; Cyclodextrin based pharmaceutics: past, present and future. Nat Rev Drug Discov; 2004; 3: 1023-1035.

[53] Szejtli J, Szente L; Elimination of bitter, disgusting tastes of drugs and foods by cyclodextrins. Eur J Pharm Biopharm; 2005; 61: 115-125.

[54] Al-Ghananeem AM, Traboulsi AA, Dittert LW, Hussain AA; Targeted brain delivery of 17 beta-estradiol via nasally administered water soluble prodrugs. AAPS PharmSciTech; 2002; 3: E5.

[55] Mester U, Lohmann C, Pleyer U, Steinkamp G, Volcker E, Kruger H, Raj PS; A comparison of two different formulations of diclofenac sodium 0.1% in the treatment of inflammation following cataract-intraocular lens surgery. Drugs R D; 2002; 3: 143-151.

[56] Higuchi T, Connors KA; Phase-solubility techniques. Adv Anal Chem Instrum; 1965; 4: 117-212.

[57] Coleman AW, Nicolis J, Keller N, Dalbiez JP; Aggregation of cyclodextrins: an explanation of the abnormal solubility of β-cyclodextrin J Incl Phenom Mol Recog Chem; 1992; 13: 139-143.

[58] González-Gaitano G, Prodríguez P, Isasi JR, Fuentes M, Tardajos G, Sánchez M; The aggregation of cyclodextrins as studied by photon correlation spectroscopy. J Incl Phenom Macrocycl Chem; 2002; 44: 101-105.

[59] Bonini M, Rossi S, Karlsson G, Almgren M, Lo Nostro P, Baglioni P; Self-assembly of beta-cyclodextrin in water. Part 1: Cryo-TEM and dynamic and static light scattering. Langmuir; 2006; 22: 1478-1484.

[60] Loftsson T, Masson M, Brewster ME; Self-association of cyclodextrins and cyclodextrin complexes. Journal of pharmaceutical sciences; 2004; 93: 1091-1099.

[61] Yancey PG, Rodrigueza WV, Kilsdonk EP, Stoudt GW, Johnson WJ, Phillips MC, Rothblat GH; Cellular cholesterol efflux mediated by cyclodextrins. Demonstration Of kinetic pools and mechanism of efflux. The Journal of biological chemistry; 1996; 271: 16026-16034.

[62] Irie T, Uekama K; Pharmaceutical applications of cyclodextrins. III. Toxicological issues and safety evaluation. Journal of pharmaceutical sciences; 1997; 86: 147-162.

[63] Kilsdonk EP, Yancey PG, Stoudt GW, Bangerter FW, Johnson WJ, Phillips MC, Rothblat GH; Cellular cholesterol efflux mediated by cyclodextrins. The Journal of biological chemistry; 1995; 270: 17250-17256.

[64] Christian AE, Haynes MP, Phillips MC, Rothblat GH; Use of cyclodextrins for manipulating cellular cholesterol content. Journal of lipid research; 1997; 38: 2264-2272.

[65] Burckbuchler V, Wintgens V, Lecomte S, Percot A, Leborgne C, Danos O, Kichler A, Amiel C; DNA compaction into new DNA vectors based on cyclodextrin polymer: surface enhanced Raman spectroscopy characterization. Biopolymers; 2006; 81: 360-370.

[66] Galant C, Amiel C, Auvray L; Ternary complex formation in aqueous solution between a beta-cyclodextrin polymer, a cationic surfactant and DNA. Macromol Biosci; 2005; 5: 1057-1065.

[67] Cryan SA, Holohan A, Donohue R, Darcy R, O'Driscoll CM; Cell transfection with polycationic cyclodextrin vectors. Eur J Pharm Sci; 2004; 21: 625-633.

[68] Boulmedarat L, Bochot A, Lesieur S, Fattal E; Evaluation of buccal methyl-beta-cyclodextrin toxicity on human oral epithelial cell culture model. Journal of pharmaceutical sciences; 2005; 94: 1300-1309.

[69] Hovgaard L, Brondsted H; Drug delivery studies in Caco-2 monolayers. IV. Absorption enhancer effects of cyclodextrins. Pharmaceutical research; 1995; 12: 1328-1332.

[70] Agu RU, Jorissen M, Willems T, Van den Mooter G, Kinget R, Verbeke N, Augustijns P; Safety assessment of selected cyclodextrins - effect on ciliary activity using a human cell suspension culture model exhibiting in vitro ciliogenesis. International journal of pharmaceutics; 2000; 193: 219-226.

[71] Zetasizer Nano User Manual; 2007; chapter 14.

[72] Voigt R, Fahr A; Pharmazeutische Technologie. Deutscher Apotheker Verlag, Stuttgart; 2005; Chapter 2: 49-50.

[73] Zetasizer Nano User Manual; 2007; chapter 16.

[74] Voigt R, Fahr A; Pharmazeutische Technologie. Deutscher Apotheker Verlag, Stuttgart; 2005; Chapter 19: 453-455.

[75] Almgren M, Edwards K, Karlsson G; Cryo transmission electron microscopy of liposomes and related structures. Colloids Surf A: Physicochem Engineering Asp; 2000; 174: 3-21.

[76] Tang MX, Szoka FC; The influence of polymer structure on the interactions of cationic polymers with DNA and morphology of the resulting complexes. Gene therapy; 1997; 4: 823-832.

[77] Dunlap DD, Maggi A, Soria MR, Monaco L; Nanoscopic structure of DNA condensed for gene delivery. Nucleic acids research; 1997; 25: 3095-3101.

Declaration of originality

I hereby declare that this diploma is my own work and has not been submitted in any form before. Information derived from the published and unpublished work of others has been acknowledged in the text and a list of references is given in the bibliography.

Hiermit versichere ich, an Eides statt die vorliegende Arbeit selbstständig und unter ausschließlicher Verwendung der angegebenen Literatur und Hilfsmittel erstellt zu haben.
Die Arbeit wurde bisher in gleicher oder ähnlicher Form keiner anderen Prüfungsbehörde vorgelegt und auch nicht veröffentlicht.

…… ……

Katharina Leucht